Journal of Econometrics 217 (2020) 411–430

Contents lists available at ScienceDirect

Journal of Econometrics

journal homepage: www.elsevier.com/locate/jeconom

Multivariate leverage effects and realized semicovariance GARCH models

Tim Bollerslev [a,b,c,*], Andrew J. Patton [a], Rogier Quaedvlieg [d]

[a] Department of Economics, Duke University, United States
[b] NBER, United States
[c] CREATES, Denmark
[d] Erasmus School of Economics, Erasmus University Rotterdam, Netherlands

ARTICLE INFO

Article history:
Available online 23 January 2020

JEL classification:
C22
C51
C53
C58

Keywords:
High-frequency data
Realized volatility
Realized correlation
Semivariance
Asymmetric dependence

ABSTRACT

We propose new asymmetric multivariate volatility models. The models exploit estimates of variances and covariances based on the *signs* of high-frequency returns, measures known as realized semivariances, semicovariances, and semicorrelations, to allow for more nuanced responses to positive and negative return shocks than threshold "leverage effect" terms traditionally used in the literature. Our empirical implementations of the new models, including extensions of widely-used bivariate GARCH specifications for a number of individual stocks and the aggregate market portfolio as well as larger dimensional dynamic conditional correlation type formulations for a cross-section of individual stocks, provide clear evidence of improved model fit and reveal new and interesting asymmetric joint dynamic dependencies.

1. Introduction

We are grateful for the opportunity to contribute to this special issue in honor of Luc Bauwens. Bauwens has made many contributions in econometrics, including to the literature on multivariate GARCH models, asymmetric volatility dependencies, and the use of high-frequency financial data, as exemplified by Bauwens and Giot (2000), Bauwens and Laurent (2005), Bauwens et al. (2006, 2013) and Bauwens and Otranto (2016).

We build on the work of Bauwens, and others, and propose new methods to capture asymmetric responses of variances, covariances, and correlations to returns. Our new multivariate volatility models exploit estimates of variances and covariances that take into account the *signs* of high-frequency returns, measures known as realized semivariances, semicovariances, and semicorrelations, which allow for more refined responses to positive and negative return shocks than traditional binary threshold-based procedures. Applying the new models to a cross-section of U.S. equities, we demonstrate clear evidence of improved in- and out-of-sample fit compared with existing bivariate models for each of the individual stocks and the aggregate market, as well as in larger-dimensional dynamic conditional correlation type formulations. We also uncover new and interesting dynamic dependencies and asymmetric news responses not accounted for by the models hitherto analyzed in the literature.

It has long been recognized that financial markets react differently to positive and negative news. In particular, volatility tends to increase more following negative return shocks than after equally-sized positive shocks. One possible explanation

* Correspondence to: Department of Economics, Duke University, 213 Social Sciences Building, Box 90097, Durham, NC 27708-0097, United States.
E-mail address: boller@duke.edu (T. Bollerslev).

https://doi.org/10.1016/j.jeconom.2019.12.011
0304-4076/

for this phenomenon, originally proposed by Black (1976), is financial leverage. Although this explanation has long been discredited as the sole explanation for the observed asymmetries (see, e.g., the discussions in Bollerslev et al., 2006; Aït-Sahalia et al., 2013), the term "leverage effect" has stuck, and it is now commonly used to refer to any volatility model, univariate and multivariate alike, in which the (co)variances respond asymmetrically to positive and negative shocks. We will follow suit, and use this term similarly below.

The first GARCH-type models that allowed for a "leverage effect" are the threshold formulations proposed independently by Glosten et al. (1993) and Zakoïan (1994). Multivariate extensions were subsequently put forth by De Goeij and Marquering (2004), McAleer et al. (2009) and Francq and Zakoïan (2012) in which the conditional (co)variances are allowed to react differently to differently signed return innovations (we will refer to all of these models as GJR-type formulations for brevity).[1] Closely related multivariate formulations based on extensions of the DCC model (Engle, 2002) to allow for threshold effects in conditional correlations have explored by Cappiello et al. (2006) and Audrino and Trojani (2011). Despite these developments, the way in which volatility asymmetries manifest in multivariate settings remains fairly poorly understood, and the recent surveys by Rombouts et al. (2014) and de Almeida et al. (2018) both explicitly call for additional research into more flexible and empirically realistic asymmetric multivariate specifications.

Meanwhile, another large and growing strand of the literature has emphasized the advantages of using high-frequency data when conducting inference about financial market volatility more generally, and ex-post volatility measures in particular (see, e.g. Andersen et al., 2013). In response to this, realized volatility measures constructed from high-frequency data have been incorporated into more traditional GARCH-type models for daily and lower frequency return volatilities as a way to enhance the informational efficiency of the models. The univariate and multivariate HEAVY models of Shephard and Sheppard (2010) and Noureldin et al. (2012), respectively, provide a prominent example of this approach. None of these models, however, include any asymmetric response terms. The univariate and multivariate Realized GARCH models of Hansen et al. (2012, 2014), respectively, do allow for "leverage effects", but only in the traditional threshold sense in which the volatility may react differently to positive and negative daily, or longer horizon, return innovations.

Set against this background, we propose a new class of multivariate realized GARCH models, where the asymmetry depends not on the sign of the daily return, but on the signs of the *intradaily* returns. More specifically, we allow heterogeneous responses of future variances and covariances to realized measures associated with signed high-frequency returns. In the univariate context this amounts to decomposing realized variance into positive and negative realized semivariances (as originally proposed by Barndorff-Nielsen et al., 2010) and dynamic models involving these measures (as previously explored by Patton and Sheppard, 2015, among others). Bollerslev et al. (2019) provide a natural generalization of this idea to a multivariate context, by decomposing the realized covariances into four separate realized semicovariance components: two based on concordant signed high-frequency returns and two based on discordant signed high-frequency returns. Further building on that idea, the new multivariate realized GARCH models proposed here explicitly utilize realized semivariances, semicovariances, and semicorrelations in modeling the dynamic dependencies in conditional covariance matrices.

The new realized semicovariance-based models thus provide a more natural "continuous" rather than "threshold" description of the widely-used return-volatility asymmetries, or "leverage effects". Existing asymmetric volatility models effectively portray the total daily variation as arising from either "good" or "bad" news, as identified by positive or negative daily returns. Correspondingly, the proportional impact of the lagged daily variation measures, whether based on realized volatility measures or not, is restricted to one of two values in the univariate setting, or one of three or four values in the multivariate setting. In contrast, the new models proposed here explicitly recognize that the fraction of the total variation stemming from positive and negative high-frequency returns generally is not binary, and in turn allow for more flexible "continuous leverage effects" and less rigid news response functions and surfaces. This additional flexibility in turn results in statistically significant improvements over existing asymmetric volatility models that effectively ignore the signs of the intraday returns.

Our empirical analysis is based on a data set comprised of high-frequency intraday data for 24 individual U.S. equities as well as the S&P 500 aggregate market index. To illustrate the usefulness of the new methods, we consider both bivariate models for each of the 24 stocks and the market index, and 24-dimensional joint models for all of the stocks. We choose to rely on relatively simple and widely-used bivariate scalar models and DCC-type formulations, but the same basic ideas may be extended to allow for non-scalar parameter matrices, more complicated component structures, or regime-switching models (see, e.g., Bauwens et al., 2016, 2017, or Bauwens and Otrando, 2018). Our empirical results suggest that while the GJR threshold specifications commonly used in the literature work quite well in the univariate setting, the new "continuous leverage" specifications result in significantly better fitting multivariate models. This improvement in the fit of the new models may be directly attributed to the existence of more complicated dynamic dependencies and asymmetries in the data beyond those accounted for by conventional threshold-based asymmetric volatility models.

The remainder of this paper is organized as follows. Section 2 briefly reviews the new realized semicovariance measures and discusses their use in the formulation of bivariate asymmetric volatility models. Section 3 describes our data. The empirical results pertaining to the bivariate models are presented in Section 4. Section 5 discusses the results from larger-dimensional DCC-type models involving realized semicorrelations. Section 6 concludes. Technical proofs and more detailed discussions, along with additional empirical results, are presented in Appendix.

[1] The EGARCH model of Nelson (1991) also allows for asymmetric responses to past return shocks, but that model does not easily generalize to a multivariate setting, and accordingly it has not been used nearly as widely as the GJR type formulations for modeling dynamic conditional covariance matrices.

2. Realized semicovariances and multivariate volatility modeling

We begin this section with a brief discussion of the realized semicovariance measures, followed by a description of the different types of models that we implement in our empirical analysis.

2.1. Realized covariances and semicovariances

Let $r_{t,k,i}$ denote the return over the kth ($k = 1, \ldots, m$) equally-spaced intradaily time-interval on day t ($t = 1, \ldots, T$) for asset i ($i = 1, \ldots, N$). Further, let the corresponding vector of returns for the N assets be denoted by $\mathbf{r}_{t,k} \equiv \left[r_{t,k,1}, \ldots, r_{t,k,N}\right]'$. The realized covariance matrix for day t (see, e.g., Barndorff-Nielsen and Shephard, 2004) is then defined by summing the m outer products of the high-frequency return vectors ($\mathbf{r}_{t,k}\mathbf{r}_{t,k}'$) over that day. To illustrate, consider the bivariate case corresponding to $N = 2$,

$$\mathbf{RCOV}_t \equiv \sum_{k=1}^{m} \mathbf{r}_{t,k}\mathbf{r}_{t,k}' = \begin{bmatrix} RV_{t,1} & RCOV_t \\ RCOV_t & RV_{t,2} \end{bmatrix}. \tag{1}$$

Extending the realized semivariance concept first proposed by Barndorff-Nielsen et al. (2010) to a multivariate setting, Bollerslev et al. (2019) suggest further decomposing $\mathbf{RCOV}_t$ into four separate realized semicovariance components based on the signs of the underlying high-frequency returns.

In particular, let $\mathbf{r}_{t,k}^{+}$ and $\mathbf{r}_{t,k}^{-}$ denote the vectors of signed positive and negative high-frequency returns.[2] The "concordant" bivariate realized semicovariance matrices associated with the bivariate realized covariance matrix in (1) are defined as,[3]

$$\begin{aligned} \mathbf{P}_t &\equiv \sum_{k=1}^{m} \mathbf{r}_{t,k}^{+}\,\mathbf{r}_{t,k}^{+\prime} = \begin{bmatrix} \mathcal{V}_{t,1}^{+} & \mathcal{P}_t \\ \mathcal{P}_t & \mathcal{V}_{t,2}^{+} \end{bmatrix}, \\ \mathbf{N}_t &\equiv \sum_{k=1}^{m} \mathbf{r}_{t,k}^{-}\,\mathbf{r}_{t,k}^{-\prime} = \begin{bmatrix} \mathcal{V}_{t,1}^{-} & \mathcal{N}_t \\ \mathcal{N}_t & \mathcal{V}_{t,2}^{-} \end{bmatrix}, \end{aligned} \tag{2}$$

while the "discordant" semicovariance matrices are defined as,

$$\begin{aligned} \mathbf{M}_t^{+} &\equiv \sum_{k=1}^{m} \mathbf{r}_{t,k}^{+}\,\mathbf{r}_{t,k}^{-\prime} = \begin{bmatrix} 0 & \mathcal{M}_t^{-} \\ \mathcal{M}_t^{+} & 0 \end{bmatrix}, \\ \mathbf{M}_t^{-} &\equiv \sum_{k=1}^{m} \mathbf{r}_{t,k}^{-}\,\mathbf{r}_{t,k}^{+\prime} = \begin{bmatrix} 0 & \mathcal{M}_t^{+} \\ \mathcal{M}_t^{-} & 0 \end{bmatrix}. \end{aligned} \tag{3}$$

The concordant realized semicovariance matrices, $\mathbf{P}_t$ and $\mathbf{N}_t$, are thus comprised of the positive and negative realized semivariances, $\mathcal{V}_t^{+}$ and $\mathcal{V}_t^{-}$, on their diagonals, and the scalar realized semicovariances, $\mathcal{P}_t$ and $\mathcal{N}_t$, on the off-diagonal. The discordant realized semicovariance matrices, $\mathbf{M}_t^{+}$ and $\mathbf{M}_t^{-}$, have zeros on their diagonals and the scalar realized semicovariances, $\mathcal{M}_t^{+}$ and $\mathcal{M}_t^{-}$, on the off-diagonals. It follows readily from the above definitions that $\mathbf{RCOV}_t = \mathbf{P}_t + \mathbf{N}_t + \mathbf{M}_t^{+} + \mathbf{M}_t^{-}$, and that $\mathbf{M}_t^{+} = \mathbf{M}_t^{-\prime}$. Moreover, when the ordering of the assets is arbitrary, the two discordant semicovariance matrices are naturally combined into a single matrix, $\mathbf{M}_t \equiv \mathbf{M}_t^{+} + \mathbf{M}_t^{-}$.

2.2. Semicovariance-based multivariate GARCH models

To more formally set up the different models, let $\mathbf{r}_t = [r_{t,1}, \ldots, r_{t,N}]'$ denote the vector of daily returns (or daily residuals from some model for the conditional mean), and $\mathbf{H}_t$ the corresponding $N \times N$ conditional covariance matrix. That is,

$$\mathbf{r}_t = \mathbf{H}_t^{1/2}\mathbf{z}_t, \tag{4}$$

where $\mathbf{z}_t$ denotes a vector of conditionally serially uncorrelated, but not necessarily *i.i.d.*, innovations with identity covariance matrix. We rely QMLE estimation techniques for making inference about all of the different models for $\mathbf{H}_t$, as further justified in Appendix C.

---

[2] Formally, $\mathbf{r}_{t,k}^{+} \equiv \mathbf{r}_{t,k} \odot \mathbf{I}_{t,k}^{+}$ and $\mathbf{r}_{t,k}^{-} \equiv \mathbf{r}_{t,k} \odot \mathbf{I}_{t,k}^{-}$, where $\odot$ denotes the Hadamard (element-by-element) product, and $\mathbf{I}_{t,k}^{+} \equiv \left[\mathbf{1}_{\{r_{t,k,1}>0\}}, \ldots, \mathbf{1}_{\{r_{t,k,N}>0\}}\right]'$ and $\mathbf{I}_{t,k}^{-} \equiv \left[\mathbf{1}_{\{r_{t,k,1}\leq 0\}}, \ldots, \mathbf{1}_{\{r_{t,k,N}\leq 0\}}\right]'$.

[3] These definitions readily extend to $N > 2$.

We take the popular "scalar" bivariate GARCH model as a our starting point. This particular formulation may be seen as a special case of both the "vech-GARCH" model of Bollerslev et al. (1988) and the "BEKK" model of Engle and Kroner (1995). In line with recent work, we estimate the intercept matrix using "covariance targeting",

$$\mathbf{H}_t = (1-\alpha-\beta)\bar{\mathbf{H}} + \beta\mathbf{H}_{t-1} + \alpha\mathbf{r}_{t-1}\mathbf{r}_{t-1}', \tag{5}$$

replacing the $\bar{\mathbf{H}}$ matrix with the sample covariance matrix of $\mathbf{r}_t$.[4] The α and β parameters are both assumed to be scalar, but richer parameterizations could, of course, be entertained.

The simple scalar model in (5) directly mirrors the widely-used univariate GARCH model of Bollerslev (1986). Meanwhile, following Noureldin et al. (2012) and Hansen et al. (2014), the availability of high-frequency data allows us to replace the noisy estimate of the conditional covariance matrix provided by the outer-product of the daily return vectors with a more accurate realized covariance matrix,[5]

$$\mathbf{H}_t = (1-\alpha^*-\beta)\bar{\mathbf{H}} + \beta\mathbf{H}_{t-1} + \alpha\mathbf{RCOV}_{t-1}, \tag{6}$$

where $\alpha^* \equiv \alpha \times \overline{\mathbf{RCOV}} \times \bar{\mathbf{H}}^{-1}$, and $\overline{\mathbf{RCOV}}$ is computed as the time series mean of $\mathbf{RCOV}_t$. The parameter α^* serves to equate the unconditional level of $\mathbf{RCOV}_t$ with the covariance of the daily returns. We will adjust the definition of α^* for the various models we consider below accordingly.[6]

Exploiting the decomposition of the realized covariance matrix into its realized semicovariance components described in Section 2.1, the multivariate realized GARCH model defined in (6) is naturally extended to allow for different parameters associated with the different realized semicovariance components,

$$\mathbf{H}_t = (1-\alpha^*-\beta)\bar{\mathbf{H}} + \beta\mathbf{H}_{t-1} + \alpha^P\mathbf{P}_{t-1} + \alpha^N\mathbf{N}_{t-1} + \alpha^M\mathbf{M}_{t-1}, \tag{7}$$

where $\alpha^* \equiv (\alpha^P\bar{\mathbf{P}} + \alpha^N\bar{\mathbf{N}} + \alpha^M\bar{\mathbf{M}}) \times \bar{\mathbf{H}}^{-1}$, and the $\bar{\mathbf{P}}$, $\bar{\mathbf{N}}$, and $\bar{\mathbf{M}}$ matrices are estimated by the time series means of $\mathbf{P}_t$, $\mathbf{N}_t$, and $\mathbf{M}_t$, respectively. By allowing the α^P, α^N, and α^M parameters to be different, this model permits the semicovariance matrices to differently impact the future covariance matrix, and in turn allows for asymmetries stemming from differently signed high-frequency returns. In light of existing evidence pertaining to the "leverage effect", one might naturally expect that negative returns would result in higher future volatilities than positive returns, and accordingly that the estimate for α^N would be greater than the estimates for both α^P and α^M. Of course, if the different semicovariance matrices have the same impact on the future covariance matrix, then $\alpha^P = \alpha^N = \alpha^M$ and the model reduces to the realized GARCH model in Eq. (6).

The model defined in (7) combines the effect of the two discordant realized semicovariance matrices into a single discordant matrix, $\mathbf{M}_t$. When the ordering of the assets is important (e.g., when modeling the returns on an individual asset and the market, as in our bivariate models estimated below), the above model may reasonably be improved by splitting the discordant semicovariance matrix into its two individual components,

$$\begin{aligned}\mathbf{H}_t = {} & (1-\alpha^*-\beta)\bar{\mathbf{H}} + \beta\mathbf{H}_{t-1} \\ & + \alpha^P\mathbf{P}_{t-1} + \alpha^N\mathbf{N}_{t-1} + \alpha^{M+}\mathcal{T}(\mathbf{M}^+_{t-1}) + \alpha^{M-}\mathcal{T}(\mathbf{M}^-_{t-1}),\end{aligned} \tag{8}$$

where $\alpha^* \equiv (\alpha^P\bar{\mathbf{P}}+\alpha^N\bar{\mathbf{N}}+\alpha^{M+}\mathcal{T}(\bar{\mathbf{M}}^+)+\alpha^{M-}\mathcal{T}(\bar{\mathbf{M}}^-)) \times \bar{\mathbf{H}}^{-1}$, and the $\mathcal{T}(\cdot)$ operator sets the lower triangular part of a matrix equal to its upper triangular part.[7] This ensures that the $\mathcal{T}(\mathbf{M}^+_{t-1})$ and $\mathcal{T}(\mathbf{M}^-_{t-1})$ matrices each contain unique information, and that the resulting $\mathbf{H}_t$ matrix symmetric. While the $\mathcal{T}(\mathbf{M}^{+/-}_t)$ matrices are symmetric, they are not positive definite, as their diagonal elements are zero. Correspondingly, parameter restrictions that ensure positive definiteness of $\mathbf{H}_t$ are not readily available, but such restrictions are easily imposed during the estimation on the filtered volatility path.

In the next section we further connect the new realized semicovariance-based models defined above to traditional threshold-based asymmetric multivariate volatility models.

2.3. Traditional asymmetric multivariate GARCH models

It is instructive to compare and contrast the new models introduced in the previous section to some of the multivariate volatility models previously used in the literature to account for asymmetric dependencies, or "leverage effects". Most of these already existing procedures rely on extensions of the univariate GJR (Glosten et al., 1993) threshold approach to

[4] In recent work, Frazier and Renault (2016) proposed a more efficient two-step estimation procedure instead of using the sample covariance matrix for $\bar{\mathbf{H}}$, and Engle et al. (2019) advocated the use of non-linear shrinkage procedures for improved estimation of $\bar{\mathbf{H}}$ in large dimensions.

[5] Noureldin et al. (2012) and Hansen et al. (2014) refer to this as a HEAVY and Realized GARCH model, respectively. Our specification is purposely simpler than the specifications employed in both of those studies, in that we do not include an auxiliary model for the dynamics of $\mathbf{RCOV}_t$. Such a specification would be necessary for the calculation of multi-step-ahead forecasts.

[6] This is especially important when daily returns are measured close-to-close, while the realized measures are based on open-to-close returns only.

[7] Formally, $\mathcal{T}(\mathbf{A}) \equiv ivech(vech(\mathbf{A}'))$, with $vech$ defined as the half-vec operator, which stacks the lower triangle of a matrix into a column vector, and $ivech$ as its inverse, leading to a symmetric matrix. This transformation has previously been used by He and Teräsvirta (2002) and De Goeij and Marquering (2004) to convert an asymmetric matrix into a symmetric matrix.

allow the conditional covariance matrix to respond differently to the cross-products of lagged daily returns depending on the signs of the returns (prominent examples include Kroner and Ng, 1998; De Goeij and Marquering, 2004; McAleer et al., 2009; Francq and Zakoïan, 2012). Alternatively, only the conditional variances are explicitly allowed to respond asymmetrically to past returns, with any asymmetries in the covariances indirectly inferred from auxiliary assumptions about the conditional correlations, as in the CCC (Bollerslev, 1990) and DCC (Engle, 2002) models.

To illustrate the former, and most direct, approach, let $\mathbf{r}_t^+$ and $\mathbf{r}_t^-$ denote the vector of signed daily positive and negative returns, respectively.[8] A straightforward multivariate generalization of the univariate GJR model with covariance targeting that does not depend on the ordering of the assets is then given by,

$$\begin{aligned}\mathbf{H}_t = &(1-\alpha^*-\beta)\bar{\mathbf{H}} + \beta\mathbf{H}_{t-1} \\ &+ \alpha^P\mathbf{r}_{t-1}^+\mathbf{r}_{t-1}^{+'} + \alpha^N\mathbf{r}_{t-1}^-\mathbf{r}_{t-1}^{-'} + \alpha^M(\mathbf{r}_{t-1}^+\mathbf{r}_{t-1}^{-'} + \mathbf{r}_{t-1}^-\mathbf{r}_{t-1}^{+'}),\end{aligned} \tag{9}$$

where $\alpha^* \equiv (\alpha^P\bar{\mathbf{H}}^P + \alpha^N\bar{\mathbf{H}}^N + \alpha^M\bar{\mathbf{H}}^M) \times \bar{\mathbf{H}}^{-1}$, and $\bar{\mathbf{H}}^P \equiv \frac{1}{T}\sum_{t=1}^T \mathbf{r}_t^+\mathbf{r}_t^{+'}$, with $\bar{\mathbf{H}}^N$ and $\bar{\mathbf{H}}^M$ defined analogously.

As discussed above, in some situations the ordering of the assets does matter. In that situation the sum of the mixed cross-products of the returns is naturally decomposed into two separate terms, necessitating the use of the $\mathcal{T}(\cdot)$ operator to render the conditional covariance matrix defined by the model symmetric,

$$\begin{aligned}\mathbf{H}_t = &\ (1-\alpha^*-\beta)\bar{\mathbf{H}} + \beta\mathbf{H}_{t-1} \\ &+ \alpha^P\mathbf{r}_{t-1}^+\mathbf{r}_{t-1}^{+'} + \alpha^N\mathbf{r}_{t-1}^-\mathbf{r}_{t-1}^{-'} + \alpha^{M+}\mathcal{T}(\mathbf{r}_{t-1}^+\mathbf{r}_{t-1}^{-'}) + \alpha^{M-}\mathcal{T}(\mathbf{r}_{t-1}^-\mathbf{r}_{t-1}^{+'}),\end{aligned} \tag{10}$$

where $\alpha^* \equiv (\alpha^P\bar{\mathbf{H}}^P + \alpha^N\bar{\mathbf{H}}^N + \alpha^{M+}\bar{\mathbf{H}}^{M+} + \alpha^{M-}\bar{\mathbf{H}}^{M-}) \times \bar{\mathbf{H}}$, and $\bar{\mathbf{H}}^{M+} \equiv \frac{1}{T}\sum_{t=1}^T \mathcal{T}(\mathbf{r}_t^+\mathbf{r}_t^{-'})$, with $\bar{\mathbf{H}}^{M-}$ defined analogously. A version of this model was first estimated by De Goeij and Marquering (2004).

The multivariate asymmetric volatility models defined in (9) and (10) do not utilize any high-frequency information. Meanwhile, extending the realized GARCH model in (6), which does incorporate high-frequency information, to allow for asymmetries in the way in which the conditional covariance matrix responds to positive and negative lagged daily returns along the lines of the model in (9), readily suggests the following specification,

$$\begin{aligned}\mathbf{H}_t = &\ (1-\alpha^*-\beta)\bar{\mathbf{H}} + \beta\mathbf{H}_{t-1} \\ &+ \left(\alpha^P\mathbf{I}_t^+\mathbf{I}_t^{+'} + \alpha^N\mathbf{I}_t^-\mathbf{I}_t^{-'} + \alpha^M(\mathbf{I}_t^+\mathbf{I}_t^{-'} + \mathbf{I}_t^-\mathbf{I}_t^{+'})\right) \odot \mathbf{RCOV}_{t-1},\end{aligned} \tag{11}$$

where $\alpha^* \equiv (\alpha^P\overline{\mathbf{RCOV}}^P + \alpha^N\overline{\mathbf{RCOV}}^N + \alpha^M\overline{\mathbf{RCOV}}^M) \times \bar{\mathbf{H}}^{-1}$, $\overline{\mathbf{RCOV}}^P \equiv \frac{1}{T}\sum_{t=1}^T \mathbf{RCOV}_t \odot \mathbf{I}_t^+\mathbf{I}_t^{+'}$, with $\overline{\mathbf{RCOV}}^N$ and $\overline{\mathbf{RCOV}}^M$ defined analogously to $\overline{\mathbf{RCOV}}^P$. A closely related asymmetric formulation has recently been estimated by Anatolyev and Kobotaev (2018). Comparing the asymmetric realized volatility model in (11) to the new realized semicovariance-based model in (7), allows for a direct assessment of the additional information provided by the signed high-frequency returns compared to that of the signed daily returns.[9]

To further appreciate this connection between the models in which the asymmetry is dictated by the signs of the daily returns only and the new models based on the realized semicovariances, suppose that the spot volatility is constant. Under this simplifying assumption it can be shown that,

$$\mathbf{P}_t \approx \mathbf{RCOV}_t \odot \left[\frac{1}{m}\sum_{k=1}^m \mathbf{I}_{t,k}^+\mathbf{I}_{t,k}^{+'}\right] \equiv \mathbf{RCOV}_t \odot \bar{\mathbf{I}}_t^P, \tag{12}$$

with similar expressions holding true for the other realized semicovariances. Thus, in this situation the right-hand-side approximation to the realized semicovariances directly mirrors the right-hand-side explanatory variables in the model in (11), except that the binary indicators for the daily returns are replaced with averages of m indicators for the high-frequency returns. In the extreme case when all of the intraday returns have the same sign, the models in (11) and (7) are therefore equivalent. However, in all other situations, the model in (7) based on the realized semicovariances affords a more nuanced response based on the proportion of the daily variation associated with specifically signed intradaily return pairs. In particular, substituting the approximation in Eq. (12) into the model in (7),

$$\mathbf{H}_t \approx (1-\alpha^*-\beta)\bar{\mathbf{H}} + \beta\mathbf{H}_{t-1} + \left(\alpha^P\bar{\mathbf{I}}_{t-1}^P + \alpha^N\bar{\mathbf{I}}_{t-1}^N + \alpha^M\bar{\mathbf{I}}_{t-1}^M\right) \odot \mathbf{RCOV}_{t-1}.$$

While in the traditional threshold asymmetric model, the impact of $\mathbf{RCOV}_{t-1}$ is either α^P, α^N or α^M, in the realized semicovariance-based model, its impact is instead determined by a weighted sum of these parameters, with the weights depending on the *proportion* of high frequency returns that are jointly positive, negative, or of mixed signs.

[8] These are the daily analogs of the high frequency signed returns discussed in Section 2.1. Formally, $\mathbf{r}_t^+ \equiv \mathbf{r}_t \odot \mathbf{I}_t^+$ and $\mathbf{r}_t^- \equiv \mathbf{r}_t \odot \mathbf{I}_t^-$, where $\mathbf{I}_t^+ \equiv \left[\mathbf{1}_{\{r_{t,1}>0\}}, \ldots, \mathbf{1}_{\{r_{t,N}>0\}}\right]'$ and $\mathbf{I}_t^- \equiv \left[\mathbf{1}_{\{r_{t,1}\leq 0\}}, \ldots, \mathbf{1}_{\{r_{t,N}\leq 0\}}\right]'$ denote indicator vectors for the signs of the daily returns.

[9] In parallel to the models defined in (8) and (10), in some situations it may be natural to include the $\mathbf{I}_t^+\mathbf{I}_t^{-'}$ and $\mathbf{I}_t^-\mathbf{I}_t^{+'}$ terms separately.

Table 1
Descriptive statistics.

	RV	$\mathcal{V}^+$	$\mathcal{V}^-$	$RCOV$	$\mathcal{P}$	$\mathcal{N}$	$\mathcal{M}^+$	$\mathcal{M}^-$	$\sigma(\mathcal{V}^+)$	$\sigma(\mathcal{P})$	$\sigma(\mathcal{M}^+)$
Market	1.134	0.568	0.566						0.215		
AAPL	2.272	1.118	1.154	0.988	0.545	0.545	−0.049	−0.053	0.210	0.225	0.104
BA	6.119	3.023	3.096	1.445	0.815	0.804	−0.091	−0.083	0.216	0.226	0.193
CAT	3.464	1.711	1.753	1.098	0.633	0.620	−0.078	−0.078	0.224	0.235	0.140
CSCO	4.049	1.983	2.066	1.329	0.733	0.727	−0.064	−0.067	0.216	0.228	0.128
CVX	2.527	1.264	1.263	1.019	0.572	0.569	−0.059	−0.063	0.216	0.232	0.110
DD	5.311	2.632	2.679	1.543	0.833	0.830	−0.061	−0.059	0.209	0.225	0.132
DIS	1.895	0.954	0.940	0.719	0.433	0.429	−0.070	−0.073	0.203	0.229	0.131
GE	3.326	1.653	1.673	1.203	0.666	0.662	−0.061	−0.064	0.210	0.227	0.133
GS	3.664	1.819	1.845	1.369	0.737	0.727	−0.045	−0.051	0.211	0.227	0.108
HD	4.844	2.390	2.454	1.414	0.782	0.777	−0.071	−0.074	0.219	0.230	0.187
IBM	3.732	1.820	1.912	1.224	0.694	0.668	−0.067	−0.071	0.210	0.229	0.123
INTC	4.977	2.470	2.507	1.544	0.831	0.824	−0.056	−0.054	0.210	0.223	0.139
KO	2.496	1.236	1.260	1.059	0.578	0.576	−0.047	−0.048	0.212	0.226	0.097
MCD	2.534	1.258	1.276	0.793	0.479	0.473	−0.079	−0.080	0.208	0.228	0.133
MMM	2.818	1.385	1.433	0.886	0.537	0.518	−0.084	−0.085	0.215	0.234	0.157
MRK	3.255	1.594	1.660	1.253	0.678	0.672	−0.049	−0.048	0.207	0.225	0.099
MSFT	3.271	1.604	1.667	0.938	0.566	0.550	−0.090	−0.088	0.212	0.232	0.176
NKE	2.705	1.353	1.352	0.920	0.534	0.537	−0.078	−0.073	0.204	0.230	0.153
PFE	1.718	0.854	0.864	0.678	0.407	0.407	−0.068	−0.068	0.200	0.228	0.125
PG	3.288	1.598	1.690	0.970	0.577	0.565	−0.086	−0.086	0.218	0.238	0.189
TRV	2.874	1.416	1.458	1.080	0.607	0.593	−0.059	−0.060	0.217	0.233	0.122
UTX	2.771	1.384	1.387	0.956	0.553	0.543	−0.070	−0.070	0.212	0.231	0.124
VZ	2.418	1.206	1.211	0.890	0.508	0.505	−0.062	−0.060	0.208	0.226	0.135
WMT	3.523	1.746	1.777	1.154	0.655	0.645	−0.072	−0.074	0.213	0.232	0.142

Note: This table provides descriptive statistics for our dataset of 24 Dow Jones Industrial Average Stocks. The top row provides statistics for the S&P500 index, while each of the other rows presents statistics for the individual stocks. The first two panels of columns report the time-series averages of the realized (co)variances and realized semi(co)variances. The final panel reports the time-series standard deviation of the ratio of its argument to the sum of itself and its opposite sign equivalent, i.e., $\sigma(\mathcal{V}^+) = StDev(\mathcal{V}_t^+/(\mathcal{V}_t^+ + \mathcal{V}_t^-))$, $\sigma(\mathcal{P}) = StDev(\mathcal{P}_t/(\mathcal{P}_t + \mathcal{N}_t))$, and $\sigma(\mathcal{M}^+) = StDev(\mathcal{M}_t^+/(\mathcal{M}_t^+ + \mathcal{M}_t^-))$.

3. Data description

Our sample consists of the 24 constituents of the Dow Jones Industrial Average that traded continuously over the period January 1, 2000 to December 31, 2014, a total of 3773 days, together with a value-weighted S&P 500 market index over the same time period. Guided by the need to balance theoretical efficiency gains from sampling returns at ever-higher frequencies with practical considerations of market microstructure effects, we rely 15-minute returns in the construction of all the realized (semi)covariance matrices.

Summary statistics for the different measures are reported in Table 1. The first three columns report the average daily realized variance, RV, and realized semivariances, $\mathcal{V}^+$ and $\mathcal{V}^-$. The averages for the S&P 500 market portfolio are reported in the first row, with the results for each of the individual stocks the subsequent 24 rows. The middle five columns show the average daily realized covariance between each of the individual stocks and the market index, $RCOV$, as well as its decomposition into the four realized semicovariance components, labeled $\mathcal{P}$, $\mathcal{N}$, $\mathcal{M}^+$ and $\mathcal{M}^-$. As the table shows, the average values of the realized semivariances, and concordant and discordant realized semicovariance pairs, are each very close.

However, while the averages of the semivariances, and pairs of semicovariances are almost equal, they can differ quite substantially on any given day. To reveal this, the final three columns report the empirical standard deviation of the ratio of their argument to the sum of its pair; i.e., $\sigma(\mathcal{V}^+) = StDev(\mathcal{V}_t^+/(\mathcal{V}_t^+ + \mathcal{V}_t^-))$, $\sigma(\mathcal{P}) = StDev(\mathcal{P}_t/(\mathcal{P}_t + \mathcal{N}_t))$, and $\sigma(\mathcal{M}^+) = StDev(\mathcal{M}_t^+/(\mathcal{M}_t^+ + \mathcal{M}_t^-))$. If the magnitudes of the different realized semi(co)variance pairs were indeed the same over time, the ratios should be identically equal to 0.5, and their standard deviations correspondingly equal to zero. Meanwhile, the numbers in the table indicate considerable time-series variation, with an average standard deviation in excess of 0.2 for the semivariances and slightly higher for the concordant semicovariances.

This temporal variation in the relative values of the semivariances and semicovariances is fundamentally what motivates the new asymmetric volatility models described in the previous section; by allowing for different coefficients for the different realized semicovariance components, the models exploit price fluctuations throughout the day, rather than implicitly treating the aforementioned ratios as being constant.

4. Bivariate volatility models

The multivariate volatility models discussed in Section 2 can in principle be implemented in any dimension. However, it is well known that the practical estimation of multivariate GARCH-type models present a host of formidable challenges in larger dimensions (see, e.g., the discussion in Bauwens et al., 2016). Hence, we focus our initial empirical analysis and illustration of the new models on bivariate applications, in which we estimate two-dimensional models for each of the

Table 2
Bivariate GARCH model estimates: Disney and S&P 500.

	BG	tBG	rBG	trBG	crBG	tBG-S	trBG-S	crBG-S
β	0.943	0.946	0.699	0.774	0.741	0.946	0.774	0.751
	(0.005)	(0.005)	(0.037)	(0.031)	(0.028)	(0.005)	(0.028)	(0.026)
α	0.050		0.217					
	(0.004)		(0.026)					
α^P		0.011		0.133	0.061	0.011	0.130	0.049
		(0.004)		(0.020)	(0.024)	(0.004)	(0.019)	(0.023)
α^N		0.083		0.207	0.393	0.082	0.211	0.390
		(0.006)		(0.025)	(0.040)	(0.006)	(0.024)	(0.037)
α^M		0.031		0.218	−0.109			
		(0.006)		(0.021)	(0.028)			
α^{M+}						0.041	0.207	0.272
						(0.014)	(0.022)	(0.078)
α^{M-}						0.022	0.230	−0.483
						(0.014)	(0.022)	(0.073)
$\mathcal{L}$	−11176	−11109	−11083	−11064	−11008	−11109	−11063	−10996

Note: This table provides parameter estimates and standard errors (in parentheses) for the bivariate GARCH (BG) models between Walt Disney Company and the S&P 500. BG refers to the simple scalar model defined in Eq. (5), while tBG, rBG, trBG and crBG refer to the generalizations in Eqs. (9), (6), (11) and (7), respectively. The models labeled with an **-S** refer to the specifications where the discordant covariance terms enter the model separately.

24 stocks together with the S&P 500 market portfolio. We subsequently consider 24-dimensional models for all of the stocks based on parsimonious DCC-type specifications explicitly designed to handle larger dimensions.

4.1. Bivariate GARCH model estimates

We begin by considering the more detailed estimation results for a single representative stock, Disney. The results reported in the first five columns of Table 2 all pertain to models which involve the combined discordant return matrices ($\mathbf{r}_t^+\mathbf{r}_t^{-\prime}+\mathbf{r}_t^-\mathbf{r}_t^{+\prime}$ or $\mathbf{M}_t \equiv \mathbf{M}_t^+ + \mathbf{M}_t^-$) only. The estimates reveal three distinct features. Firstly, consistent with a large existing literature in financial econometrics, high-frequency information clearly improves the fit of the models: the symmetric realized Bivariate GARCH model (rBG) improves on the standard Bivariate GARCH (BG) model by 93 likelihood points, with no change in the number of estimated parameters. Secondly, adding low frequency asymmetry terms significantly improves the fit of the model: the daily and high-frequency threshold versions of the previous models (tBG and trBG) show gains of 67 and 19 likelihood points, respectively, well beyond conventional critical values required with the two additional parameters. Thirdly, comparing the new realized semicovariance-based model that effectively allow for continuous asymmetry (crBG) with the threshold realized GARCH model (trBG) results in a gain of 56 likelihood points, with no change in the number of estimated parameters. As such, this clearly underscores the informational advantages afforded by the use of the new realized semicovariances in explaining the asymmetries compared to the more traditional threshold-based asymmetric models.

The last three columns of the table further investigates whether splitting up the discordant matrices into the two separate components provides any additional useful information compared with the models that only include their sum. Comparing the "split" models (labeled with an -S in the table) with their "non-split" counterparts reveals little to no evidence of an improvement in fit for the models that rely on the traditional binary daily threshold to determine the split (tBG-S and trBG-S). However, the fit of the new semicovariance-based model is significantly improved by splitting the discordant semicovariance matrix into two: the "split" model (crBG-S) beats the "non-split" model (crBG) by 12 likelihood points, well beyond the critical value required for a single additional parameter. When judged by the value of the likelihood, this final model also provides the by far best overall fit among all the models.

Table 3 summarizes the estimation results for the same set of models for all of the 24 stocks. The table reports the average parameter estimates across stocks, along with the cross-sectional 10% and 90% quantiles in square brackets. The average log-likelihood across all stocks is given below the parameter estimates. The table reveals the same general set of conclusions as the specific estimates for Disney in Table 2. The use of realized volatility measures significantly improves the fit of the models. The inclusion of asymmetry terms further enhances the fit, with the realized semicovariance-based models providing greatest improvements. Splitting the discordant terms based on the signed daily returns results in fairly minor improvements on average, while the gains from splitting the discordant realized semicovariance $\mathbf{M}$ into $\mathbf{M}^+$ and $\mathbf{M}^-$ again appears larger.

Buttressing these conclusions, the row marked *#LR* reports the 10% rejection frequencies of a likelihood ratio test between the "split" and "non-split" models. While splitting up the discordant terms leads to improvements for about a quarter of the 24 stocks when the split is based on daily thresholds (tBG-S and trBG-S), the improvements observed for the "continuous" asymmetric models that split the discordant realized semicovariances (crBG-S) are significant for just over half of the stocks.

Table 3
Bivariate GARCH model estimates: DJIA Individual Stocks and S&P 500.

	BG	tBG	rBG	trBG	crBG	tBG-S	trBG-S	crBG-S
β	0.941	0.941	0.739	0.776	0.766	0.941	0.778	0.770
	[0.931:0.949]	[0.933:0.950]	[0.641:0.812]	[0.689:0.841]	[0.682:0.820]	[0.933:0.950]	[0.695:0.845]	[0.684:0.822]
α	0.052		0.217					
	[0.046:0.059]		[0.169:0.303]					
α^P		0.014		0.147	0.087	0.014	0.145	0.079
		[0.008:0.020]		[0.093:0.215]	[0.019:0.178]	[0.008:0.020]	[0.090:0.214]	[0.011:0.173]
α^N		0.085		0.233	0.337	0.085	0.232	0.340
		[0.075:0.097]		[0:186:0.315]	[0.282:0.426]	[0.075:0.098]	[0.184:0.313]	[0.283:0.427]
α^M		0.040		0.213	0.031			
		[0.026:0.052]		[0.154:0.289]	[-0.082:0.138]			
α^{M+}						0.034	0.204	0.160
						[0.008:0.060]	[0.137:0.289]	[-0.077:0.333]
α^{M-}						0.045	0.222	−0.102
						[0.023:0.067]	[0.155:0.296]	[-0.342:0.114]
$\mathcal{L}$	−11113	−11052	−11007	−10988	−10965	−11051	−10986	−10962
#LR-test						6	7	13
Rivers and Vuong (2002) test:								
crBG	24	22	23	13		21	13	
crBG-S	24	22	24	15		22	14	

Note: This table provides a summary of parameter estimates for the bivariate GARCH models for each of the 24 DJIA stocks and the S&P 500. BG refers to the simple scalar model defined in Eq. (5), while tBG, rBG, trBG and crBG refer to the generalizations in Eqs. (9), (6), (11) and (7), respectively. The models labeled with a **-S** refer to the specification where the discordant terms are split into two. The table presents the average parameter estimates across all stocks, along with the 10% and 90% empirical quantiles in brackets. $\mathcal{L}$ gives the average likelihood across models. The bottom panel contains tests comparing significance of in-sample fit. The first row presents the number of series for which a Likelihood Ratio test between the split and non-split models is significant at the 10%-level. The bottom two rows consider the in-sample test of Rivers and Vuong (2002) for non-nested models. The second-last (last) row presents the number of stocks for which the crBG (crBG-S) model fits significantly better than the model in that column at the 10%-level.

In contrast to the split and non-split models, which are easily compared, all of the other models in the table are non-nested, which complicates any head-to-head comparisons of their likelihoods. The bottom two rows in the table present the results of the Rivers and Vuong (2002) test for comparing in-sample fit of non-nested models. In particular, comparing the realized semicovariance-based models (crBG and crBG-S) to the other models, the table shows that the new models improves significantly on the fit of the already existing asymmetric volatility models for the vast majority of the stocks. The only exception is the threshold realized-GARCH models (trBG and trBG-S), for which the non-nested tests in favor of the continuous asymmetric models are only significant for about half the stocks. (We note, however, that the Rivers and Vuong, 2002 test *never* finds that the threshold models provide a significantly better fit than the new continuous asymmetry model.).

4.2. News impact surfaces and impulse response functions

It is instructive to consider the implications of the actual parameter estimates to help understand the relative performance of the different models discussed. Looking first at the traditional low frequency threshold model (tBG), there is clear evidence of asymmetry, as manifest by $\alpha^N > \alpha^M > \alpha^P$: joint positive returns have the smallest impact on the future covariance matrix, while joint negative returns have the largest effect. This, of course, is directly in line with the celebrated "leverage effect", and explains why multivariate volatility models that allow for asymmetry are generally preferred.

The larger α estimates obtained for the realized models (rBG and trBG) also directly corroborate the existing realized volatility literature: since **RCOV** provides a more precise estimate of covariation than the outer product of the daily returns, the need for "smoothing" is reduced and larger α estimates and more rapidly responding models are thereby obtained. The ordering of the parameter estimates for the realized threshold model (trBG) directly mirrors that of the daily threshold model (tBG), but the coefficients are larger, again because **RCOV** is a more precise measure of covariation. The new continuous asymmetry model (crBG) has an even larger α^N and stronger reaction to joint negative return variation. At the same time, the estimates for α^P and α^M are both lower than for the realized threshold model (trBG). Even on days when the daily returns are positive, a large proportion of the total daily variation may still stem from joint negative intraday returns, resulting in inflated coefficients for $\mathbf{P}_t$ and $\mathbf{M}_t$ for the traditional realized threshold model, which does not exploit information on the signs of high frequency returns.

The estimates for α^P and α^N for the split models, reported in the last three columns of Table 3, are all fairly close to those for the corresponding non-split models. This is also true for the α^{M+} and α^{M-} estimates for the daily threshold models (tBG-S and trBG-S), which are both fairly close to the estimates for α^M for the corresponding non-split models (tBG and trBG), implying little gain from splitting up the discordant matrix. Interestingly, however, there is a much larger difference between the two coefficients for the new continuous asymmetric split model (crBG-S), and the estimates are

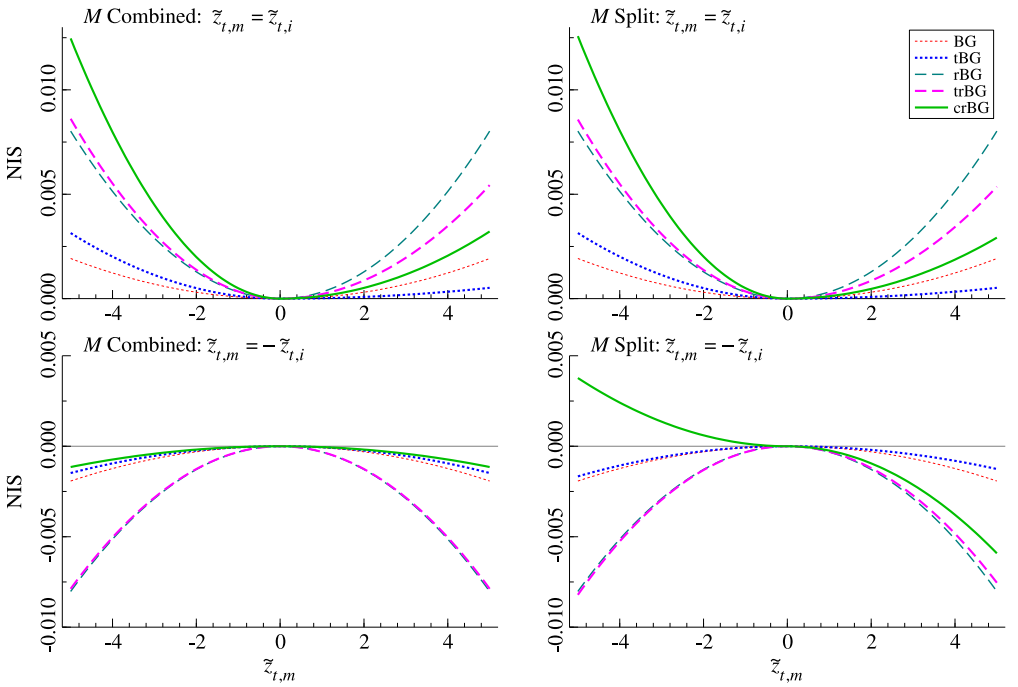

Fig. 1. News Impact Surfaces. *Note:* The four panels present cross-sections of the News Impact Surface for the covariance element $H_{t,mi}$. They are based on the average parameter estimates in Table 3. The left column gives the results for the models where the discordant covariance elements are combined. The right column represents the models in which they are split. The top row shows the slices for $z_{t,m} = z_{t,i}$, while the bottom row depicts the slices for $z_{t,m} = -z_{t,i}$.

also of the opposite sign: the α^{M-} coefficient is *negative*. This negative estimate, combined with the fact that $\mathcal{T}(\mathbf{M}^-)$ is always non-positive, implies that variation stemming from negative market returns combined with positive stock returns tends to *increase* the correlation between the asset and the market. Conversely, on days with positive intraday market returns and negative intraday stock returns, correlations tend to decrease, as manifest by the positive α^{M+} coefficient multiplied by the non-positive $\mathcal{T}(\mathbf{M}^+)$. This additional flexibility afforded by the new models is also consistent with the empirical regularity that correlations tend to increase (decrease) in overall bear (bull) markets.

To further visualize these differences in the way in which the models respond to new information, Fig. 1 shows a series of News Impact Surfaces (NIS) (following the definition of Engle and Ng, 1993). More specifically, we plot the reaction of the off-diagonal element $H_{mi,t+1}$ to differently sized shocks based on the average parameter estimates for each of the different models reported in Table 3. To allow for easy interpretation, rather than plotting the full surface for a range of shocks, we only plot the news impact curves for $\tilde{z}_{t,m} = \tilde{z}_{t,i}$ and $\tilde{z}_{t,m} = -\tilde{z}_{t,i}$, corresponding to slices along the main and secondary diagonals of the full news impact surface. Additional details concerning the actual computation of these NISs, along with a discussion of the subtleties involved in defining NIS for models that use both high-frequency and daily data, are outlined in Appendix B.

Looking first at the top row, the figure shows the impact of same-signed return shocks, with the NISs for the non-split models in the left panel and the results for the split models in the right panel. Since the NISs for same-signed shocks only depend on the α^P and α^N parameters, and the estimates for these parameters are very similar across the split and non-split models, the two plots appear almost identical. Meanwhile, there is clear evidence for asymmetries, or "leverage effects", and most strongly so in the new realized semicovariance-based model (crBG): that model has both a lower response to joint positive shocks, and a higher response to joint negative shocks then any of the other realized models.

The bottom row displays the NISs for opposite-signed return shocks, as a function of the market return shock, $\tilde{z}_{t,m}$. The results for the non-split models shown in the left panel all imply a symmetric response to positive and negative mixed shocks, with the conventional realized models exhibiting the largest effects. Somewhat surprisingly, the new realized semicovariance based model (crBG) exhibits the lowest response to oppositely signed shocks among all of the models. The results for the split models in the right panel help explain why. The continuous asymmetric split model (crBG-S) is the only model to unveil a clear asymmetry in the response to mixed-signed shocks: when $\tilde{z}_{t,m}$ is negative, future covariances tend to go *up*, while the response to positive $\tilde{z}_{t,m}$ closely mirrors that of the other realized models. None of the other models reveal this more nuanced asymmetry.

The NISs only speak to the immediate one-day-ahead response to differently sized and signed shocks. Non-linear Impulse Response Functions (IRFs) (originally proposed by Gallant et al., 1993) provide a framework for understanding

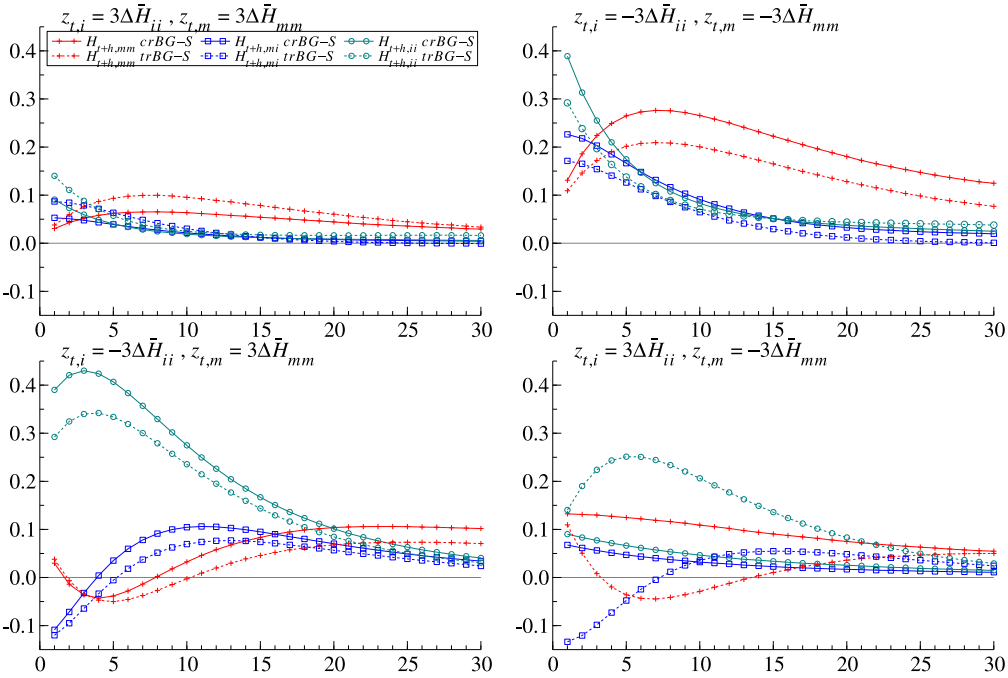

Fig. 2. Impulse Response Functions. *Note:* The four panels present the Impulse Response Functions (IRF) for four different shock combinations, for each of the covariance elements, based on the average parameter estimates in Table 3. The solid lines represent the IRFs for the continuous asymmetry model (crBG-S) defined in (7), while the dashed lines give the IRFs for corresponding split version of the threshold realized model (trBG-S) defined in (11).

the longer-run dynamic implications of the different models by tracing out the responses to differently sized shocks through the use of Monte Carlo simulation techniques for calculating and comparing $\mathbb{E}[\mathbf{H}_{t+h}|\mathcal{F}_t, \mathbf{z}_t]$ to the benchmark case obtained for $\mathbf{z}_t \equiv 0$. Fig. 2 reports the resulting IRFs up to a 30-day horizon for the four different elements of the covariance matrix, for the threshold realized covariance-based model that allow for a split response (trBG-S: dashed lines) and the new continuous asymmetry model based on the realized semicovariances (crBG-S: solid lines). The four panels report the results for four different initial shock combinations, $\tilde{z}_t = (\tilde{z}_{t,m}, \tilde{z}_{t,i})$. Further details concerning the actual calculations are provided in Appendix B.

Looking first at the results in the top row for the same-signed shocks, the variances and covariances both increase. This, of course, is to be expected from the widely-documented persistent volatility clustering phenomenon. The basic patterns also appear fairly similar for the two different shock pairs, albeit almost three times as large for the negative shocks in the right panel. This discrepancy in the responses is the largest for the new continuous model. In both cases, however, the shocks have the greatest initial impact on the individual stock volatility, but after a few periods the volatility of the market starts to rise and exhibits the greatest overall persistence.

Turning to the bottom row, and the IRFs for the mixed-signed shocks, reveal more pronounced differences between the continuous and threshold models. A negative shock to the individual stock, depicted in the lower left panel, results in a large increase in its volatility, and a temporary decrease in the covariance with the market. Also, this effect appears slightly stronger for the continuous model. Meanwhile, a negative market shock, shown in the bottom right panel, results in distinctly differently shaped IRFs for the two different models. For the threshold model, the impact is qualitatively similar to that of a negative individual stock shock shown in the bottom left panel, with an increase in the variance of the market, and a decrease in the covariance. For the continuous asymmetry model, however, there is an immediate increase in the covariance, as well as the two variances, all of which then gradually decline over time. Again, this more nuanced response stems directly from the use of the separate realized semicovariance components in the formulation and estimation of the new crBG-S model.

4.3. Out-of-sample forecasts

The results discussed in the previous sections naturally raise the question: do the improved in-sample fit and the more complicated dependencies afforded by the new models translate into improved out-of-sample forecast performance? To answer this question, we re-estimate all of the models every 20th observation based on rolling sample windows of

Table 4
Bivariate GARCH models: Out-of-sample loss.

	Frobenius	MCS	QLIKE	MCS
BG	21.681	0.000	1.869	0.000
tBG	18.811	0.000	1.841	0.458
rBG	18.307	0.125	1.895	0.000
trBG	17.950	0.042	1.903	0.000
crBG	17.029	0.417	1.850	0.583
tBG-S	18.647	0.167	1.848	0.125
trBG-S	17.899	0.125	1.910	0.000
crBG-S	17.022	0.625	1.858	0.125

Note: The table presents the out-of-sample Frobenius and QLIKE loss of the various models, averaged across time and stocks. The columns labeled MCS present the fraction of stocks for which the model is included in the 80% Model Confidence Set of Hansen et al. (2011). BG refers to the simple scalar model defined in Eq. (5), while tBG, rBG, trBG and crBG refer to the generalizations in Eqs. (9), (6), (11) and (7), respectively. The **-S** models refer to the specifications where the discordant terms are split into two.

1000 observations, resulting in a total of 2773 out-of-sample forecast observations. We evaluate the forecasts using the Frobenius distance and QLIKE loss with respect to the ex-post $\mathbf{RCOV}_t$,

$$Frobenius_t = \sqrt{\text{Tr}(\mathbf{H}_t - \mathbf{RCOV}_t)(\mathbf{H}_t - \mathbf{RCOV}_t)'}, \tag{13}$$

and,

$$QLIKE_t = \log|\mathbf{H}_t| + \text{Tr}(\mathbf{H}_t^{-1}\mathbf{RCOV}_t), \tag{14}$$

where $\mathbf{H}_t$ refers to the forecast produced by the different models (Patton, 2011, and Rombouts et al., 2013, provide formal justifications for these two loss functions).

Table 4 summarizes the resulting out-of-sample forecast loss, averaged across time and stocks.[10]. In terms of the Frobenius distance, the split version of the continuous asymmetric model (crBG-S) has the lowest loss, closely followed by its non-split counterpart (crBG). The standard threshold model that only uses daily information (tBG), does surprisingly well in terms of QLIKE loss, performing on par with the two continuous asymmetric models.

In order to test whether the differences in forecast loss are statistically significant, we also implement the Model Confidence Set (MCS) of Hansen et al. (2011). The MCS procedure selects a set of models that contains the best model with a certain probability, here set to 80%. Based on the Frobenius distance, either, or both, of the continuous asymmetric models (crBG and crBG-S) are included in the MCS for all but four of the stocks. The split continuous asymmetric model is also the model included in most of the confidence sets. For the QLIKE loss the continuous asymmetric model (crBG) is the model most often included in the MCS, although again somewhat surprisingly the traditional daily threshold model is included in almost half of the MCSs. All-in-all, the forecasting results essentially underscore the conclusions drawn from the in-sample estimates: the new realized semicovariance based models that allow for richer asymmetric dependencies perform the best.

5. High-dimensional multivariate volatility models

Traditional bivariate GARCH models, and the extensions thereof incorporating the realized semicovariance measures, such as those considered above, do not easily scale to large dimensions. Alternatively, the Dynamic Conditional Correlation (DCC) model of Engle (2002), in which the conditional variances and the conditional correlations are modeled separately, has emerged as a popular and easy-to-implement framework for capturing the dynamic dependencies in larger dimensional conditional covariance matrices. In this section we consider extensions of DCC type models based on the new realized semicovariance measures. We begin by defining new realized semicorrelations, followed by a discussion of the new DCC formulations that we use in our joint modeling of the 24 individual stocks included in our sample.

5.1. Realized correlations and semicorrelations

Realized correlations are naturally defined from the realized covariance matrix as (see, e.g., Barndorff-Nielsen and Shephard, 2004),

$$\mathbf{RCOR}_t \equiv \text{diag}\left(\mathbf{RCOV}_t\right)^{-1/2} \cdot \mathbf{RCOV}_t \cdot \text{diag}\left(\mathbf{RCOV}_t\right)^{-1/2}, \tag{15}$$

where diag$(\cdot)$ denotes the operator that sets the off-diagonal elements of a matrix to zero. This same definition readily extends to the concordant realized semicovariance matrices. In particular, since $\mathbf{P}_t$ and $\mathbf{N}_t$ are both defined as sums of

[10] Average losses for each of the individual stocks are presented in the Supplemental Appendix

outer-products of high-frequency return vectors, they are by definition both positive semi-definite. Hence, provided none of the realized semivariances along the diagonals are zero, which is true empirically for all of the stocks and days in our sample, this naturally suggests the following definitions of the positive and negative semicorrelation matrices,

$$\mathbf{R}_t^P \equiv \text{diag}\,(\mathbf{P}_t)^{-1/2} \cdot \mathbf{P_t} \cdot \text{diag}\,(\mathbf{P}_t)^{-1/2}, \tag{16}$$

$$\mathbf{R}_t^N \equiv \text{diag}\,(\mathbf{N}_t)^{-1/2} \cdot \mathbf{N_t} \cdot \text{diag}\,(\mathbf{N}_t)^{-1/2}, \tag{17}$$

with representative elements,

$$R_{t,ij}^P = \frac{\mathcal{P}_{t,ij}}{\sqrt{\mathcal{V}_{t,i}^+ \mathcal{V}_{t,j}^+}}, \qquad R_{t,ij}^N = \frac{\mathcal{N}_{t,ij}}{\sqrt{\mathcal{V}_{t,i}^- \mathcal{V}_{t,j}^-}}. \tag{18}$$

That is, the positive (negative) semicovariance is normalized by the square-root of the product of positive (negative) semivariances, directly mirroring the usual definition of a correlation.

The definition of mixed realized semicorrelations is a bit more subtle, as the discordant semicovariance matrices, $\mathbf{M}_t^+$ and $\mathbf{M}_t^-$, and thus also $\mathbf{M}_t$, have zeros along the diagonal. In Appendix A we show that normalizing the discordant realized semicovariance matrix by the realized variances guarantees that the resulting mixed semicorrelations are bounded by one in absolute value, and that this bound is tight, in the sense that it is the weakest normalization that ensures such a bound. Correspondingly, we define the mixed semicorrelation matrix as,

$$\mathbf{R}_t^M \equiv \text{diag}\,(\mathbf{RCOV}_t)^{-1/2} \cdot \mathbf{M}_t \cdot \text{diag}\,(\mathbf{RCOV}_t)^{-1/2} + I_2, \tag{19}$$

where I_2 is the 2×2 identity matrix. $\mathbf{R}_t^M$ has typical off-diagonal element given by

$$R_{t,ij}^M = \frac{M_{t,ij}}{\sqrt{RCOV_{t,ii} RCOV_{t,jj}}} \equiv \frac{\mathcal{M}_{t,ij}}{\sqrt{\mathcal{V}_{t,i}\mathcal{V}_{t,j}}}, \qquad i \neq j, \tag{20}$$

It follows immediately from this definition that $\mathbf{R}_t^M$ is symmetric, with diagonal values equal to one, and off-diagonal values bounded by one in absolute value. However, the matrix is not necessarily positive semidefinite for $N > 2$.

If the realized semivariances are symmetric (i.e., $\mathcal{V}_{t,i}^+ = \mathcal{V}_{t,i}^- = \frac{1}{2}\mathcal{V}_{t,i}$ and $\mathcal{V}_{t,j}^+ = \mathcal{V}_{t,j}^- = \frac{1}{2}\mathcal{V}_{t,j}$), then a simple weighted average of the three semicorrelation matrices can be shown (see Appendix A) to equal the usual correlation matrix,

$$RCOR_{t,ij} = \frac{1}{2} R_{t,ij}^P + \frac{1}{2} R_{t,ij}^N + R_{t,ij}^M, \qquad i \neq j.$$

As such, the above definitions imply a decomposition of the standard realized correlation matrix into its semicorrelation components similar to the decomposition of the realized covariance matrix into its semicovariance components.

5.2. Realized semicorrelation-based DCC models

The DCC model is based on a decomposition of the conditional covariance matrix into matrices of conditional variances and correlations,

$$\mathbf{H}_t = \mathbf{D}_t \mathbf{R}_t \mathbf{D}_t, \tag{21}$$

where $\mathbf{D}_t = \text{diag}(\mathbf{H}_t)^{1/2}$. In the formulation originally proposed and estimated by Engle (2002), the elements of $\mathbf{D}_t$ are modeled using standard univariate GARCH-type specifications, while the correlation dynamics are defined through the quasi-correlation matrix $\mathbf{Q}_t$,

$$\mathbf{R}_t = \text{diag}(\mathbf{Q}_t)^{-1/2} \cdot \mathbf{Q}_t \cdot \text{diag}(\mathbf{Q}_t)^{-1/2}, \tag{22}$$

$$\mathbf{Q}_t = (1 - \alpha - \beta)\bar{\mathbf{Q}} + \beta \mathbf{Q}_{t-1} + \alpha \mathbf{z}_{t-1}\mathbf{z}_{t-1}', \tag{23}$$

where $\mathbf{z}_t \equiv \mathbf{D}_t^{-1}\mathbf{r}_t$, and $\bar{\mathbf{Q}}$ refers to the sample mean of $\mathbf{z}_t\mathbf{z}_t'$.[11] More complicated formulations with non-scaler α and β parameters may be defined in a similar manner.

In parallel to the multivariate GARCH models discussed in Section 2, the DCC model may similarly be augmented to include high-frequency information by replacing the lagged cross-product of the standardized returns with the realized correlations, as previously suggested by Bauwens et al. (2012) and Pelletier and Kassi (2014), among others. Accordingly, we define a simple realized DCC model by replacing the recursive equation for $\mathbf{Q}_t$ in Eq. (23) with,[12]

$$\mathbf{Q}_t = (1 - \alpha - \beta)\bar{\mathbf{Q}} + \beta \mathbf{Q}_{t-1} + \alpha \mathbf{RCOR}_{t-1}. \tag{24}$$

[11] Aielli (2013) instead defines $z_{t,i} = r_{t,i} q_{t,ii}^{1/2} h_{t,ii}^{-1/2}$ such that $\mathbb{E}(\mathbf{z}_t\mathbf{z}_t') = \mathbb{E}(\mathbf{Q}_t)$. This adjustment generally has little impact on the empirical properties of the model. Moreover, little is known about the theoretical properties of DCC-type models in general, and we therefore rely on the default DCC specification of Engle (2002) as our starting point.

[12] This differs from the formulation of Bauwens et al. (2012), which replaces the cross-product term with $\mathbf{V}_{t-1} = \mathbf{D}_{t-1}^{-1}\mathbf{RCOV}_{t-1}\mathbf{D}_{t-1}^{-1}$; i.e., the realized covariance scaled by the estimated conditional variances.

Decomposing the realized correlations into the semicorrelations defined above, we naturally obtain the following generalization of this realized DCC model,

$$\mathbf{Q}_t = (1-\alpha^*-\beta)\bar{\mathbf{Q}} + \beta\mathbf{Q}_{t-1} + \alpha^P\mathbf{R}^P_{t-1} + \alpha^N\mathbf{R}^N_{t-1} + \alpha^M\mathbf{R}^M_{t-1}, \tag{25}$$

where $\alpha^* \equiv (\alpha^P\bar{\mathbf{R}}^P + \alpha^N\bar{\mathbf{R}}^N + \alpha^M\bar{\mathbf{R}}^M) \times \bar{\mathbf{Q}}^{-1}$. In parallel to the realized semicovariance-based GARCH models analyzed above, the DCC model defined in (25) effectively allows for continuous asymmetry. The fact that $\mathbf{R}^M_{t-1}$ is not guaranteed to be positive definite for $N > 2$, could in principle result in the $\mathbf{Q}_t$ matrix defined in (25) being non-positive definite, especially for large values of α^M. (In our empirical application discussed below we never encountered this problem.) In practice, if need be, this could also easily be enforced during the estimation of the model.

Putting the results from the new realized semicorrelation-based DCC model into perspective, we also consider more traditional GJR-type threshold versions of the DCC model obtained by adding cross-product terms of the signed de-volatilized returns to the recursion in Eq. (23). In particular, generalizing the formulation first estimated by Cappiello et al. (2006) to include multiple such terms, we consider,

$$\begin{aligned}\mathbf{Q}_t = &(1-\alpha^*-\beta)\bar{\mathbf{Q}} + \beta\mathbf{Q}_{t-1} \\ &+ \alpha^P\mathbf{z}^+_{t-1}\mathbf{z}^{+'}_{t-1} + \alpha^N\mathbf{z}^-_{t-1}\mathbf{z}^{-'}_{t-1} + \alpha^M(\mathbf{z}^+_{t-1}\mathbf{z}^{-'}_{t-1} + \mathbf{z}^-_{t-1}\mathbf{z}^{+'}_{t-1}),\end{aligned} \tag{26}$$

where $\alpha^* \equiv (\alpha^P\bar{\mathbf{Q}}^P + \alpha^N\bar{\mathbf{Q}}^N + \alpha^M\bar{\mathbf{Q}}^M) \times \bar{\mathbf{Q}}^{-1}$, $\bar{\mathbf{Q}}^P \equiv \frac{1}{T}\sum_{t=1}^T \mathbf{z}^+_t\mathbf{z}^{+'}_t$, with $\bar{\mathbf{Q}}^N$ and $\bar{\mathbf{Q}}^M$ defined analogously.

As a final mix between this more traditional threshold DCC model and the newer generation realized DCC model, we also estimate a threshold realized DCC model,

$$\begin{aligned}\mathbf{Q}_t = &(1-\alpha^*-\beta)\bar{\mathbf{Q}} + \beta\mathbf{Q}_{t-1} + \alpha^P\mathbf{RCOR}_{t-1} \odot \mathbf{I}^+_{t-1}\mathbf{I}^{+'}_{t-1} \\ &+ \alpha^N\mathbf{RCOR}_{t-1} \odot \mathbf{I}^-_{t-1}\mathbf{I}^{-'}_{t-1} \\ &+ \alpha^M\mathbf{RCOR}_{t-1} \odot (\mathbf{I}^+_{t-1}\mathbf{I}^{-'}_{t-1} + \mathbf{I}^-_{t-1}\mathbf{I}^{+'}_{t-1}),\end{aligned} \tag{27}$$

where $\alpha^* \equiv (\alpha^P\overline{\mathbf{RCOR}}^P + \alpha^N\overline{\mathbf{RCOR}}^N + \alpha^M\overline{\mathbf{RCOR}}^M) \times \bar{\mathbf{Q}}^{-1}$, $\overline{\mathbf{RCOR}}^P \equiv \frac{1}{T}\sum_{t=1}^T \mathbf{RCOR}_t \odot \mathbf{I}^+_t\mathbf{I}^{+'}_t$, with $\overline{\mathbf{RCOR}}^N$ and $\overline{\mathbf{RCOR}}^M$ defined analogously. This final model directly mirrors the threshold realized multivariate GARCH model considered above, and helps illuminate where the improvements for the new continuous asymmetry DCC model that we document in the next section are coming from.

5.3. DCC model estimates

This section presents the results from the different DCC formulations discussed above for jointly modeling all of the 24 individual stocks. The first step consists in the estimation of univariate GARCH models for each of the stocks. In parallel to the multivariate models discussed in Section 2, we estimate conventional univariate GARCH models (Bollerslev, 1986), threshold GARCH models allowing for different responses to positive and negative daily returns (as in Glosten et al., 1993; Zakoïan, 1994), realized GARCH models (along the lines of Shephard and Sheppard, 2010; Hansen et al., 2012), threshold realized GARCH models, and continuous asymmetry realized GARCH models based on realized semivariances (similar to the models estimated by Barndorff-Nielsen et al., 2010; Chen et al., 2015).[13] A summary of the estimation results for the 24 stocks is provided in Appendix D. The threshold realized GARCH model has the highest likelihood for fourteen of the stocks, while the new continuous asymmetry realized GARCH model fits the data the best for nine of the stocks. Surprisingly, the simple threshold (GJR) GARCH model provides the best fit for one of the stocks.

Armed with the best-fitting (in terms of log-likelihood) univariate models for each of the individual stocks, we proceed to the estimation of the different DCC formulations defined above. The resulting parameter estimates reported in Table 5 are generally in line with and further corroborate the results for the corresponding bivariate model estimates for each of the individual stocks and the S&P 500 market portfolio reported in Table 3.[14] Allowing for asymmetric effects in the traditional DCC models based on daily returns (DCC compared to tDCC) increases the likelihood by 26 points, while doing so for the realized DCC models (rDCC compared to trDCC) increases the likelihood by 256 points. These estimates thus strongly support the existence of asymmetric dynamic correlation matrices, or "leverage effects" in correlations. Meanwhile, there is relatively little variation in the actual α coefficient estimates for the two threshold models. On the other hand, the estimates for the new realized semicorrelation-based model (crDCC), which has the highest overall likelihood, suggest that the mixed semicorrelations have a much smaller and less significant impact on the correlation dynamics than do the concordant semicorrelations. By comparison, the concordant negative semicovariances also had by far the largest impact in the bivariate models involving each of the individual stocks and the market.

[13] The idea of decomposing RV_t into its realized semivariance components has also been explored by Patton and Sheppard (2015) in the context of dynamic modeling using univariate HAR models.

[14] In contrast to the bivariate models involving the market as one of the two assets analyzed in Section 4, since the ordering of the 24 individual stocks is arbitrary, we do not consider the "split" versions of the models, where $\mathbf{M}^+$ and $\mathbf{M}^-$ are included separately.

Table 5
DCC model estimates for DJIA stocks.

	DCC	tDCC	rDCC	trDCC	crDCC
β	0.989	0.987	0.934	0.960	0.957
	(0.0010)	(0.0012)	(0.0047)	(0.0026)	(0.0028)
α	0.004		0.031		
	(0.0002)		(0.0020)		
α^P		0.004		0.024	0.019
		(0.0004)		(0.0017)	(0.0016)
α^N		0.007		0.028	0.021
		(0.0006)		(0.0019)	(0.0016)
α^M		0.002		0.020	0.005
		(0.0004)		(0.0014)	(0.0023)
$\mathcal{L}$	−144163	−144137	−143962	−143706	−143697

Note: The table presents parameter estimates, standard errors, and log-likelihood values for the various DCC specifications. DCC refers to the model in Eq. (23), while tDCC, rDCC, trDCC and crDCC refer to the models in Eqs. (26), (24), (27) and (25), respectively.

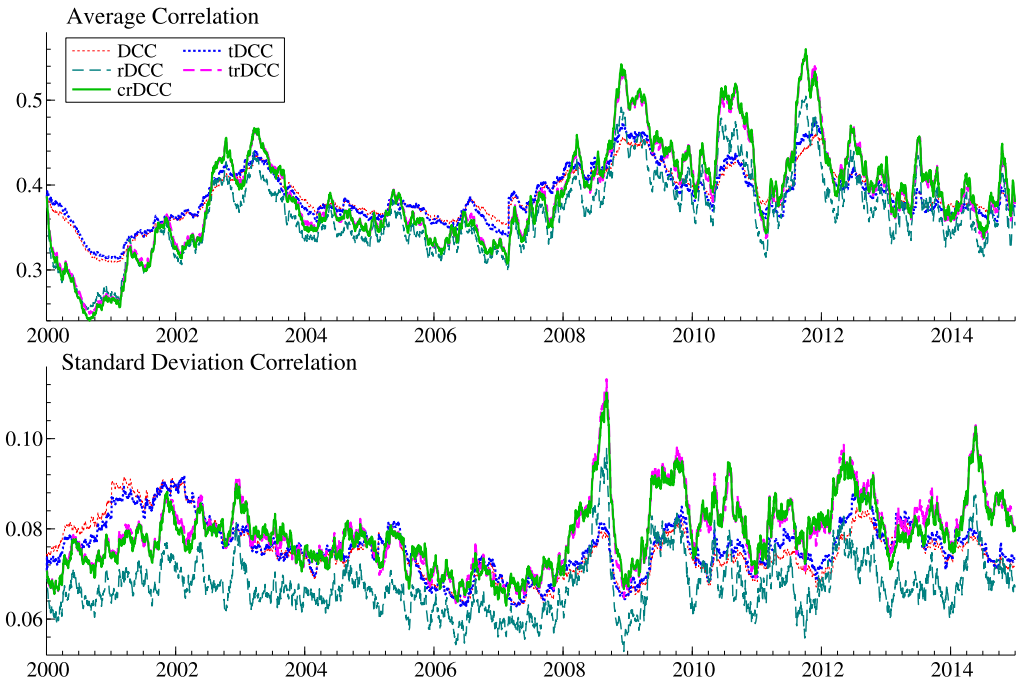

Fig. 3. DCC correlation dynamics. *Note:* The figure depicts the filtered correlation paths of the various DCC specifications. The top panel shows the average correlation across all 24 stocks, while the bottom panel shows the cross-sectional standard-deviation of the correlations over time. DCC refers to the model in Eq. (23), while tDCC, rDCC, trDCC and crDCC refer to models in Eqs. (26), (24), (27) and (25), respectively.

5.4. Correlation dynamics

To further illustrate the working of the different DCC models, Fig. 3 plots the estimated correlation paths. The top panel shows the time-series of the average pairwise correlation; i.e., $\bar{\rho}_t = \frac{2}{N(N-1)} \sum_{i>j} \rho_{ij,t}$. While the overall average correlations obtained across the different models are all fairly close and around 0.38, there are some differences in the dynamic dependencies. Most notably, the models based on realized measures seemingly exhibit the greatest variation: whereas $\bar{\rho}_t$ varies between 0.25 and 0.6 for the realized models, it remains between 0.3 and 0.45 for the traditional models that only rely on daily returns. Among the realized models, the models that explicitly allow for asymmetry (trDCC and crDCC) also appear to respond more rapidly to changing market conditions, and result in on-average higher correlations during periods of market stress and financial crisis. These visual impressions cleaned from Fig. 3, is further corroborated by the summary statistics reported in the first two columns in Table 6.

In addition to being more responsive, the asymmetric realized models also tend to exhibit larger cross-sectional variation in the estimated correlations. To underscore this, the bottom panel of Fig. 3 plots the cross-sectional standard deviation, $\sigma(\rho_t) = \sqrt{\frac{2}{N(N-1)} \sum_{i>j} (\rho_{ij,t} - \bar{\rho}_t)^2}$, over time. While the true value of $\sigma(\rho_t)$ is obviously unknown, $\sigma(\rho_t)$ provides

Table 6
DCC Correlation descriptives.

	Average $\bar{\rho}_t$	StDev $\bar{\rho}_t$	Average $\sigma(\rho_t)$
DCC	0.3869	0.0311	0.0752
tDCC	0.3866	0.0332	0.0759
rDCC	0.3655	0.0483	0.0674
trDCC	0.3867	0.0604	0.0791
crDCC	0.3866	0.0621	0.0788

Note: This table provides summary statistics pertaining to the filtered correlations from the different DCC models. DCC refers to the model in Eq. (23), while tDCC, rDCC, trDCC and crDCC refer to the models in Eqs. (26), (24), (27) and (25), respectively. $\bar{\rho}_t$ is computed as $2/(N(N-1))\sum_{i>j}\rho_{ij,t}$, while $\sigma(\rho_t) = \sqrt{2/(N(N-1))\sum_{i>j}(\rho_{ij,t} - \bar{\rho}_t)^2}$.

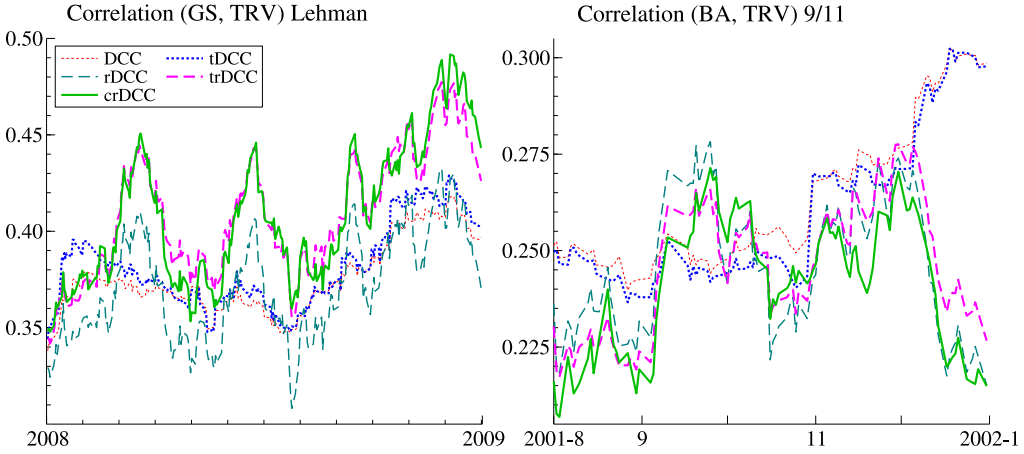

Fig. 4. DCC correlation events. *Note:* The left panel depicts the correlation between Goldman Sachs (GS) and Travelers (TRV) from January–December 2008, around the Lehman Brothers Bankruptcy and the start of the financial crisis. The right panel depicts the correlation between Boeing (BA) and Travelers (TRV) from August–December 2011, around the 9/11 terrorist attacks. DCC refers to the model in Eq. (23), while tDCC, rDCC, trDCC and crDCC refer to the models in Eqs. (26), (24), (27) and (25), respectively.

an indication of how restrictive the different parameterizations are.[15] In particular, the cross-sectional dispersion in the correlations generally appear to be larger during market turmoil, especially for the asymmetric models as most clearly evidenced by the sharp increase observed around September 2008. Interestingly, this increase in the cross-sectional dispersions start to manifest from the beginning of 2008, well before the Lehman Brothers bankruptcy on September 15, 2008. The simple realized DCC (rDCC) results in the on-average lowest cross-sectional dispersion in the estimated correlations.

To further highlight some of these differences, Fig. 4 zooms in on the estimated correlations for two specific stocks during two specific events: Goldman Sachs (GS) and Travelers (TRV) from January–December 2008, around the Lehman Brothers Bankruptcy and the start of the financial crisis (left panel), and Boeing (BA) and Travelers (TRV) from August–December 2011, around the 9/11 terrorist attacks (right panel).

Looking first at the left panel, the realized models evidently react far more quickly in predicting rising correlations. Also, the realized models that explicitly allow for asymmetry (trDCC and crDCC) both result in much higher correlations than any of the other models. Further zooming in on the figure, reveals that the continuous asymmetry model (crDCC) has slightly lower correlations than the threshold model (trDCC) pre-Lehman, but higher correlations post-Lehman.

Turning to the right panel, again shows a sharp rise in all of the correlation estimates in the immediate aftermath of 9/11. At the same time, however, the realized models and the traditional daily models completely diverge toward the end of the year, which showed a steadily recovering market, with the daily models resulting in still rising correlations, and the realized models suggesting a sharp fall. We next investigate whether these differences in the conditional correlations implied from the different models result in significantly different covariance matrix forecasts.

[15] In the extreme case, when the true latent correlations are all the same (as in the equicorrelation, or DECO, model of Engle and Kelly, 2012) $\sigma(\rho_t)$ should obviously be zero, even though model estimation error invariably will result in a value greater than zero. Conversely, even if the true correlations vary substantially over time, any model will likely miss some of that variation, in turn resulting in too small a value for $\sigma(\rho_t)$.

Table 7
DCC Models: Out-of-sample loss.

	Frobenius	MCS	QLIKE	MCS
DCC	2387.8	0.009	31.438	0.000
tDCC	2348.9	0.010	31.441	0.000
rDCC	2364.2	0.009	31.379	0.158
trDCC	2307.4	0.015	31.355	0.158
crDCC	2297.3	1.000	31.347	1.000

Note: The table presents the average out-of-sample Frobenius and QLIKE loss for the different DCC models. The columns labeled MCS present the *p*-values associated with the Model Confidence Set of Hansen et al. (2011). DCC refers to the model in Eq. (23), while tDCC, rDCC, trDCC and crDCC refer to the models in Eqs. (26), (24), (27) and (25), respectively.

5.5. Out-of-sample forecasts

We use the five different DCC models to obtain one-step-ahead out-of-sample forecasts of the 24-dimensional covariance matrix. In parallel to the bivariate GARCH out-of-sample forecasts analyzed in Section 4.3, we re-estimate the parameters of the models every 20 observations based on rolling sample windows of 1000 observations, resulting in 2773 out-of-sample forecasts.[16] We evaluate the loss associated with the covariance matrix forecasts based on the same Frobenius distance and QLIKE loss with respect to the ex-post $\mathbf{RCOV}_t$, as defined in Eqs. (13) and (14).

The resulting average losses and proportions that the various models were included in the 80% Model Confidence Sets (MCS) are reported in Table 7. The new realized semicorrelation-based model (crDCC) achieves that lowest average loss by both criteria. That same model is also included in both of the MCSs. By contrast, the probability that any one of the other models provides the best forecasts is less than 1.5% based on Frobenius' distance, and less than 16% based on QLIKE loss. As such, this strongly supports the idea that the use of the new realized semicorrelation measures proposed here can help improve the fit and the forecasting performance of existing larger-scale DCC-type models in many other practical applications.

6. Conclusion

We propose new multivariate GARCH models that exploit information from the signs of high frequency returns via measures known as realized semivariances, semicovariances, and semicorrelations. The new measures and models require no additional data beyond the high-frequency data required for the computation of conventional realized variances and covariances. The approach naturally bridges the gap that currently exist in the multivariate volatility literature between models that allow for an asymmetric reaction to positive vs. negative returns (popularly referred to as "leverage effects") and those that employ high frequency data and realized volatility measures (popularly referred to as "realized models").

The use of realized semivariances, semicovariances, and semicorrelations in essence enable the new models to accommodate "continuous", rather than "threshold" asymmetric effects. Most existing asymmetric daily volatility models classify a return as either "good" or "bad" depending on its sign, as manifest in threshold-type formulations. Our approach, on the other hand, implicitly enables the models to make use of the *proportion* of a daily return that is attributable to "good" vs. "bad" news. Correspondingly, the new models may be seen as allowing for "continuous leverage effects", thereby affording a more nuanced characterization of this salient empirical feature of equity returns.

Using data on Dow Jones individual U.S. equities and the S&P 500 market portfolio, we show that our new semicovariance-based models, which capture both the leverage effect and utilize high frequency data, significantly outperform several commonly used models that exploit only one of these features. This superior performance holds for bivariate models for the individual stocks and the aggregate market, as well as larger dimensional models for all of the individual stocks. It also holds true both in terms of in-sample fit and out-of-sample forecast accuracy.

To further elicit the covariance matrix dynamics implied by the new models, we employ "news impact surfaces" and non-linear impulse response functions. In line with past evidence, we find that joint negative returns exert a much greater impact on future covariances than joint positive returns of the same absolute magnitude. In contrast to the results based on existing models, however, the new models proposed here also delineate a distinct asymmetric reaction to opposite-signed shocks: a market downturn is typically accompanied by increasing covariances, regardless of the sign of the individual stock return.

Acknowledgments

We would like to thank Bingzhi Zhao for kindly providing us with the cleaned high-frequency data underlying our empirical investigations. Quaedvlieg was financially supported by the Netherlands Organisation for Scientific Research (NWO) Grant 451-17-009.

[16] We rely on the same individual GARCH specifications for each of the individual stocks underlying the in-sample estimation results, and we re-estimate these models using the same rolling sample scheme used in the estimation of the DCC models.

Appendix A. Mixed semicorrelations

We omit day subscripts (t) here for brevity. Recall the definition of R^M_{ij} in Eq. (20). We now prove that (a) $R^M_{t,ij} \in [-1, 0]$, and (b) these bounds are tight.

(a) Note that $\mathcal{M}_{ij}$ is weakly negative by construction, and equals zero only when all high-frequency returns are of the same sign. The upper bound for $\mathcal{M}_{ij}$ and R^M_{ij} is therefore zero. Now consider the lower bound,

$$\begin{aligned}\left|\mathcal{M}_{ij}\right| &\equiv \left|\sum_{k=1}^{m} r_{k,i}r_{k,j}\mathbf{1}_{\{r_{k,i}r_{k,j}<0\}}\right| = \sum_{k=1}^{m}\left|r_{k,i}r_{k,j}\right|\mathbf{1}_{\{r_{k,i}r_{k,j}<0\}} \\ &\leq \sum_{k=1}^{m}\left|r_{k,i}r_{k,j}\right| \leq \left(\sum_{k=1}^{m} r^2_{k,i}\sum_{k'=1}^{m} r^2_{k',j}\right)^{1/2} \equiv \sqrt{RCOV_{ii}RCOV_{jj}}.\end{aligned}$$

The first equality holds as the summands are weakly negative, the first inequality holds as the indicator is either zero or one, and the second inequality holds by Cauchy–Schwarz. Thus $0 \leq \left|R^M_{ij}\right| \leq 1$.

(b) Consider the case that $r_{k,j} = a \cdot r_{k,i}$ for some a. Assume that $a > 0$. In this case $\mathcal{M}_{ij} = 0$ since the signs of $r_{k,i}$ and $r_{k,j}$ always agree. Thus $\mathcal{M}_{ij}$ achieves its upper bound of zero under perfect positive correlation of the high-frequency returns. Now assume that $a < 0$. In this situation,

$$\begin{aligned}\mathcal{M}_{ij} &\equiv \sum_{k=1}^{m} r_{k,i}r_{k,j}\mathbf{1}_{\{r_{k,i}r_{k,j}<0\}} = \sum_{k=1}^{m} r_{k,i}r_{k,j} = a\sum_{k=1}^{m} r^2_{k,i} = a \cdot RCOV_{ii} \\ &= -\sqrt{RCOV_{ii} \cdot a^2 \cdot RCOV_{ii}} = -\sqrt{RCOV_{ii} \cdot RCOV_{jj}},\end{aligned}$$

where the first equality holds since $r_{k,i}r_{k,j} \leq 0\ \forall k$, and the last equality uses the relationship between the realized variances of the two assets. Thus the lower bound on R^M_{ij} is attained in the case of perfect negative correlation.

Next, to prove under the assumption that $\mathcal{V}^+_{t,i} = \mathcal{V}^-_{t,i} = \frac{1}{2}\mathcal{V}_{t,i}$ and $\mathcal{V}^+_{t,j} = \mathcal{V}^-_{t,j} = \frac{1}{2}\mathcal{V}_{t,j}$, note that

$$\begin{aligned}\frac{1}{2}R^P_{t,ij} + \frac{1}{2}R^N_{t,ij} + R^M_{t,ij} &\equiv \frac{\frac{1}{2}\mathcal{P}_{t,ij}}{\sqrt{\mathcal{V}^+_{t,i}\mathcal{V}^+_{t,j}}} + \frac{\frac{1}{2}\mathcal{N}_{t,ij}}{\sqrt{\mathcal{V}^-_{t,i}\mathcal{V}^-_{t,j}}} + \frac{\mathcal{M}_{t,ij}}{\sqrt{\mathcal{V}_{t,i}\mathcal{V}_{t,j}}} \\ &= \frac{\frac{1}{2}\mathcal{P}_{t,ij}}{\sqrt{\frac{1}{4}\mathcal{V}_{t,i}\mathcal{V}_{t,j}}} + \frac{\frac{1}{2}\mathcal{N}_{t,ij}}{\sqrt{\frac{1}{4}\mathcal{V}_{t,i}\mathcal{V}_{t,j}}} + \frac{\mathcal{M}_{t,ij}}{\sqrt{\mathcal{V}_{t,i}\mathcal{V}_{t,j}}} \\ &= \frac{\mathcal{P}_{t,ij} + \mathcal{N}_{t,ij} + \mathcal{M}_{t,ij}}{\sqrt{\mathcal{V}_{t,i}\mathcal{V}_{t,j}}} \\ &= \frac{RCOV_{t,ij}}{\sqrt{RCOV_{t,ii}RCOV_{t,jj}}} = RCOR_{t,ij}.\end{aligned}$$

Appendix B. Model visualization

B.1. News Impact Surfaces

The News Impact Curve (NIC) for univariate volatility models is defined as (Engle and Ng, 1993),

$$NIC(z_t) = h_{t+1}(z_t \mid h_t = \bar{h}) - h_{t+1}(0 \mid h_t = \bar{h}),$$

where z_t denotes the standardized residual, and $\bar{h}$ refers to the unconditional variance of the model. In particular, it follows readily that for a simple daily GARCH model,

$$NIC(z_t) = \alpha\bar{h}z^2_t.$$

A multivariate News Impact Surface (NIS) is naturally defined accordingly (Kroner and Ng, 1998; Asai and McAleer, 2009),

$$NIS(\mathbf{z}_t) = \mathbf{H}_{t+1}(\mathbf{z}_t \mid \mathbf{H}_t = \bar{\mathbf{H}}) - \mathbf{H}_{t+1}(\mathbf{0} \mid \mathbf{H}_t = \bar{\mathbf{H}}).$$

In order to sensibly calculate NISs for models involving realized measures based on higher-frequency intraday returns, in addition to the assumption that $\mathbf{H}_t = \bar{\mathbf{H}}$, we further assume that all of the semi(co)variances are at their unconditional levels, and that the sum of the intraday returns is zero; i.e., $\sum_{k=1}^{m}\mathbf{r}_{t,k} = \mathbf{0}$. The individual intradaily returns may still be non-zero, but requiring their sum to be zero, allows for a direct comparison of the effect of a daily shock for the models that do, and do not use any realized measures. In particular, defining the signed daily positive and negative return vectors

constructed from the high-frequency intraday returns, $\tilde{\mathbf{z}}_t^+$ and $\tilde{\mathbf{z}}_t^-$, respectively, the NISs for the split models (tBG, trBG and crBG) may be obtained as,

$$NIS(\tilde{\mathbf{z}}_t) = \alpha^P \tilde{\mathbf{z}}_t^+ \tilde{\mathbf{z}}_t^{+\prime} + \alpha^N \tilde{\mathbf{z}}_t^- \tilde{\mathbf{z}}_t^{-\prime} + \alpha^{M+} \tilde{\mathbf{z}}_t^+ \tilde{\mathbf{z}}_t^{-\prime} + \alpha^{M-} \tilde{\mathbf{z}}_t^- \tilde{\mathbf{z}}_t^{+\prime},$$

with the NISs for the simpler models obtained by appropriately restricting the parameters.

B.2. Impulse response functions

Our calculation of the Impulse Response Functions (IRFs) (Gallant et al., 1993) rely on shocks to the returns, when the process is at its unconditional average, $\bar{\mathbf{H}}$, defined as the average $\mathbf{RCOV}_t$ over the 24 pairs of stocks. Since we use a targeting specification for all of the models, α^* is based on these same averages for the semicovariances. We then simulate 1,000,000 paths of the covariance matrix for 30 days after the initial shock, to approximate $\mathbb{E}\left[\mathbf{H}_{t+h}|\mathcal{F}_t, \mathbf{z}_t = \tilde{\mathbf{z}}\right]$. The IRF is computed as the difference between the values obtained when $\tilde{\mathbf{z}} = \mathbf{z}^*$ (the shocked value for $\mathbf{z}_t$) and those when $\tilde{\mathbf{z}} = \mathbf{0}$. The paths are simulated by generating intraday 15-min returns according to the given model, assuming volatilities are constant within each trading day (though, of course, varying across days). Based on these generated returns, we obtain estimates of $\mathbf{P}_t$, $\mathbf{N}_t$, $\mathbf{M}_t^+$ and $\mathbf{M}_t^-$, which allow us to filter out the random path using the average parameter estimates in Table 3.

Appendix C. Estimation and inference

In this appendix we show consistency of a QMLE estimator for the new multivariate realized semicovariance-based GARCH specifications. Formal proofs of consistency for DCC-type models are notoriously difficult and generally unavailable, and we do not consider these models in this appendix.

We show consistency of the QMLE for the scalar bivariate GARCH version of the crBG model without covariance targeting,

$$\mathbf{H}_t = CC' + \beta \mathbf{H}_{t-1} + \alpha^P \mathbf{P}_{t-1} + \alpha^N \mathbf{N}_{t-1} + \alpha^M \mathbf{M}_{t-1}, \tag{C.1}$$

where C is a lower triangular $N \times N$ matrix with $N^* = N(N+1)/2$ parameters. Below we consider the covariance targeting version of (C.1). We assume initial values H_0 is known and positive semidefinite. Let the QML estimator $\hat{\theta} = \{C, \beta, \alpha^P, \alpha^N, \alpha^M\}$ be,

$$\hat{\theta} = \arg\max_{\theta \in \Theta} \mathcal{L}(\theta), \tag{C.2}$$

with $\mathcal{L}(\theta) = \sum_{t=1}^T l_t(\theta) = c - \log|\mathbf{H}_t| - \mathbf{r}_t' \mathbf{H}_t^{-1} \mathbf{r}_t = c - \log|\mathbf{H}_t| - tr(\mathbf{H}_t^{-1} \mathbf{Z}_t)$, where $\mathbf{Z}_t = \mathbf{r}_t \mathbf{r}_t'$.

Comte and Lieberman (2003) show strong consistency of QMLE of a BEKK-type model, of which our scalar model is a special case, by verifying conditions given in Jeantheau (1998). One of the conditions to establish strong consistency is for the model to admit a strictly stationary and ergodic solution, which we assume to be true for the crBG.

Proposition 1. *First we provide the score vectors , $S_t(\theta) = \frac{\partial l_t(\theta)}{\partial \theta'}$.*

$$S_t(\theta) = \frac{1}{2}[(\mathrm{vec}(\mathbf{Z}_t))' - (\mathrm{vec}(\mathbf{H}_t))'](\mathbf{H}_t^{-1} \otimes \mathbf{H}_t^{-1}) \frac{\partial\, \mathrm{vec}(\mathbf{H}_t)}{\partial \theta'}.$$

If the model is well specified the score vectors evaluated at the true parameter value is a martingale difference sequence with respect to $\mathcal{F}_{t-1}$.

Then, under standard regularity conditions (e.g. Comte and Lieberman, 2003), it can be shown that

$$\sqrt{T}(\hat{\theta} - \theta_0) \to_d N(0, \mathcal{I}^{-1} \mathcal{J} \mathcal{I}^{-1}), \tag{C.3}$$

where $\mathcal{J} = \mathbb{E}[S_t(\theta)' S_t(\theta)]$) and $\mathcal{I} = -\mathbb{E}\left[\frac{\partial S_t(\theta)}{\partial \theta}\right]$.

The covariance targeting version amounts to the following specification:

$$\begin{aligned} \mathbf{H}_t = {} & (\bar{\mathbf{H}}_t - \beta \bar{\mathbf{H}}_t - \alpha^P \bar{\mathbf{P}} + \alpha^N \bar{\mathbf{N}} + \alpha^M \bar{\mathbf{M}}) \\ & + \beta \mathbf{H}_{t-1} + \alpha^P \mathbf{P}_{t-1} + \alpha^N \mathbf{N}_{t-1} + \alpha^M \mathbf{M}_{t-1}. \end{aligned} \tag{C.4}$$

With covariance targeting, a two-step procedure is adopted. The score vector will no longer be a martingale difference sequence, but will have mean zero at the true parameter value. The asymptotics of the QML in this case is a direct application of two-step GMM as discussed in Newey and McFadden (1994).

Define $\tilde{l}_t(\tilde{\theta}, \bar{\mathbf{H}}, \bar{\mathbf{P}}, \bar{\mathbf{N}}, \bar{\mathbf{M}})$, where the latter four elements are estimated by a moment estimator, and $\tilde{\theta} = \{\beta, \alpha^P, \alpha^N, \alpha^M\}$ by QMLE in the second step. Estimation gives the following vector of moment conditions

$$\tilde{S}_t(\theta) = \left(\frac{\partial \tilde{l}_t}{\partial \theta'}, (\mathbf{H}_t - \bar{\mathbf{H}}), (\mathbf{P}_t - \bar{\mathbf{P}}), (\mathbf{N}_t - \bar{\mathbf{N}}), (\mathbf{M}_t - \bar{\mathbf{M}}) \right), \tag{C.5}$$

Table D.1
Univariate GARCH estimates.

	GARCH	tGARCH	rGARCH	trGARCH	crGARCH
ω	0.017	0.020	0.053	0.049	0.049
	[0.008 : 0.031]	[0.009 : 0.031]	[0.019 : 0.094]	[0.017 : 0.098]	[0.019: 0.092]
β	0.935	0.939	0.745	0.771	0.769
	[0.916 : 0.953]	[0.923 : 0.954]	[0.634 : 0.823]	[0.662 : 0.840]	[0.680 : 0.834]
α	0.061	0.023	0.226	0.157	
	[0.046 : 0.077]	[0.013 : 0.032]	[0.148 : 0.308]	[0.068 : 0.231]	
γ		0.067		0.088	
		[0.040 : 0.097]		[0.027 : 0.145]	
α^+					0.107
					[0.025 : 0.192]
α^-					0.303
					[0.212 : 0.399]
$\mathcal{L}$	−6826.49	−6805.92	−6771.81	−6764.96	−6765.47
$\#\mathcal{L}^{Max}$	0	1	0	14	9

Note: This table provides a summary of parameter estimates for the univariate GARCH models for the DJIA stocks. The table reports the average estimates across all stocks, along with the 10% and 90% empirical quantiles in brackets. $\mathcal{L}$ gives the average likelihood across models. The bottom row presents the number of stocks for which that model had the highest likelihood.

which is no longer MDS with respect to $\mathcal{F}_{t-1}$. In this case,

$$\sqrt{T}(\tilde{\theta} - \theta_0) \to_d N(0, \mathcal{I}^{-1}\mathcal{J}\mathcal{I}^{-1}), \tag{C.6}$$

where $\mathcal{J} = var[\frac{1}{\sqrt{T}}\sum_{t=1}^{T}\tilde{S}_t(\theta)]$ and

$$\mathcal{I} = -\mathbb{E}\left[\frac{\partial S_t(\theta)}{\partial\theta}\right] = -\mathbb{E}\begin{bmatrix} \frac{\partial^2\tilde{l}_t}{\partial\tilde{\mathbf{H}}\partial\theta'} & 0 & 0 & 0 & 0 \\ \frac{\partial^2\tilde{l}_t}{\partial\theta\partial\theta'} & -I_{d^*} & 0 & 0 & 0 \\ \frac{\partial^2\tilde{l}_t}{\partial\tilde{\mathbf{P}}\partial\theta'} & 0 & -I_{d^*} & 0 & 0 \\ \frac{\partial^2\tilde{l}_t}{\partial\tilde{\mathbf{N}}\partial\theta'} & 0 & 0 & -I_{d^*} & 0 \\ \frac{\partial^2\tilde{l}_t}{\partial\tilde{\mathbf{M}}\partial\theta'} & 0 & 0 & 0 & -I_{d^*}. \end{bmatrix}.$$

In the implementation we use a HAC-type estimator in place of $\mathcal{J}$.

Appendix D. Univariate GARCH estimates

We estimate the following univariate GARCH models for each of the 24 stocks, $h_{t,i} = \omega + \beta h_{t-1,i} + \alpha r^2_{t-1,i}$ (GARCH), $h_{t,i} = \omega + \beta h_{t-1,i} + \alpha r^2_{t-1,i} + \gamma r^2_{t-1,i} I\{r_{t-1,i} < 0\}$ (tGARCH), $h_{t,i} = \omega + \beta h_{t-1,i} + \alpha RV_{t-1,i}$ (rGARCH), $h_{t,i} = \omega + \beta h_{t-1,i} + \alpha RV_{t-1,i} + \gamma RV_{t-1,i} I\{r_{t-1,i} < 0\}$ (trGARCH), and $h_{t,i} = \omega + \beta h_{t-1,i} + \alpha^+ \mathcal{V}^+_{t-1,i} + \alpha^- \mathcal{V}^-_{t-1,i}$ (crGARCH). Table D.1 provides a summary of the estimation results in the form of the average parameter estimates and their cross-sectional distribution across the 24 stocks, and Table S.3 in the Supplemental Appendix provides more detailed information about the maximized likelihood values for each of the different models for each of the individual stocks.

Appendix E. Supplementary data

Supplementary material related to this article can be found online at https://doi.org/10.1016/j.jeconom.2019.12.011.

References

Aielli, G.P., 2013. Dynamic conditional correlation: On properties and estimation. J. Bus. Econom. Statist. 31 (3), 282–299.

Aït-Sahalia, Y., Fan, J., Li, Y., 2013. The leverage effect puzzle: Disentangling sources of bias at high frequency. J. Financ. Econ. 109, 224–249.

Anatolyev, S., Kobotaev, N., 2018. Modeling and forecasting realized covariance matrices with accounting for leverage. Econometric Rev. 37 (2), 114–139.

Andersen, T.G., Bollerslev, T., Christoffersen, P.C., Diebold, F.X., 2013. Financial risk measurement for financial risk management. In: Handbook of Economics of Finance, Vol. 2B. pp. 1127–1220.

Asai, M., McAleer, M., 2009. Multivariate stochastic volatility, leverage and news impact surfaces. Econometrics J. 12 (2), 292–308.

Audrino, F., Trojani, F., 2011. A general multivariate threshold GARCH model with dynamic conditional correlations. J. Bus. Econom. Statist. 29 (1), 138–149.

Barndorff-Nielsen, O.E., Kinnebrock, S., Shephard, N., 2010. Measuring downside risk: realised semivariance. In: Bollerslev, T., Russell, J., Watson, M. (Eds.), Volatility and Time Series Econometrics: Essays in Honor of Robert F. Engle. Oxford University Press, pp. 117–136.

Barndorff-Nielsen, O.E., Shephard, N., 2004. Econometric analysis of realized covariation: High frequency based covariance, regression, and correlation in financial economics. Econometrica 72 (3), 885–925.
Bauwens, L., Braione, M., Storti, G., 2017. A dynamic component model for forecasting high-dimensional realized covariance matrices. Econom. Stat. 1, 40–61.
Bauwens, L., Giot, P., 2000. The logarithmic ACD model: An application to the bid–ask quote process of three nyse stocks. Ann. Econ. Stat. 60, 117–149.
Bauwens, L., Grigoryeva, L., Ortega, J.-P., 2016. Estimation and empirical performance of non-scalar dynamic conditional correlation models. Comput. Statist. Data Anal. 100, 17–36.
Bauwens, L., Hafner, C.M., Pierret, D., 2013. Multivariate volatiliuty modeling of electricity futures. J. Appl. Econometrics 28 (5), 743–761.
Bauwens, L., Laurent, S., 2005. A new class of multivariate skew densities, with application to generalized autoregressive conditional heteroscedasticity models. J. Bus. Econom. Statist. 23 (3), 346–354.
Bauwens, L., Laurent, S., Rombouts, J.V., 2006. Multivariate GARCH models: A survey. J. Appl. Econometrics 21 (1), 79–109.
Bauwens, L., Otrando, E., 2018. Nonlinearities and regimes in conditional correlations with different dynamics. Working Paper.
Bauwens, L., Otranto, E., 2016. Modeling the dependence of conditional correlations on market volatility. J. Bus. Econom. Statist. 34 (2), 254–268.
Bauwens, L., Storti, G., Violante, F., 2012. Dynamic conditional correlation models for realized covariance matrices. Working Paper.
Black, F., 1976. Studies of stock price volatility changes. In: Proceedings of the 1976 Meetings of the American Statistical Association, pp. 171–181.
Bollerslev, T., 1986. Generalized autoregressive conditional heteroskedasticity. J. Econometrics 31, 307–327.
Bollerslev, T., 1990. Modelling the coherence in short run nominal exchange rates: A multivariate generalized ARCH model. Rev. Econ. Stat. 72 (3), 498–505.
Bollerslev, T., Engle, R.F., Wooldridge, J.M., 1988. A capital asset pricing model with time-varying covariances. J. Polit. Econ. 96 (1), 116–131.
Bollerslev, T., Li, J., Patton, A.J., Quaedvlieg, R., 2019. Realized semicovariances. Working Paper.
Bollerslev, T., Litvinova, J., Tauchen, G., 2006. Leverage and volatility feedback effects in high-frequency data. J. Financ. Econ. 4 (3), 353–384.
Cappiello, L., Engle, R.F., Sheppard, K., 2006. Asymmetric dynamics in the correlations of global equity and bond returns. J. Financ. Econ. 4 (4), 537–572.
Chen, X., Ghysels, E., Wang, F., 2015. Hybrid-garch: A generic class of models for volatility predictions using high frequency data. Statist. Sinica 759–786.
Comte, F., Lieberman, O., 2003. Asymptotic theory for multivariate GARCH processes. J. Multivariate Anal. 84 (1), 61–84.
de Almeida, D., Hotta, L.K., Ruiz, E., 2018. MGARCH models: Trade-off between feasibility and flexibility. Int. J. Forecast. 34 (1), 45–63.
De Goeij, P., Marquering, W., 2004. Modeling the conditional covariance between stock and bond returns: A multivariate GARCH approach. J. Financ. Econ. 2 (4), 531–564.
Engle, R.F., 2002. Dynamic conditional correlation: A simple class of multivariate generalized autoregressive conditional heteroskedasticity models. J. Bus. Econom. Statist. 20 (3), 339–350.
Engle, R.F., Kelly, B., 2012. Dynamic equicorrelation. J. Bus. Econom. Statist. 30 (2), 212–228.
Engle, R.F., Kroner, K.F., 1995. Multivariate simultaneous generalized ARCH. Econometric Theory 11 (1), 122–150.
Engle, R.F., Ledoit, O., Wolf, M., 2019. Large dynamic covariance matrices. J. Bus. Econom. Statist. 37 (2), 363–375.
Engle, R.F., Ng, V.K., 1993. Measuring and testing the impact of news on volatility. J. Finance 48 (5), 1749–1778.
Francq, C., Zakoïan, J.-M., 2012. QML estimation of a class of multivariate asymmetric GARCH models. Econometric Theory 28 (1), 179–206.
Frazier, D.T., Renault, E., 2016. Efficient two-step estimation via targeting. J. Econometrics 201 (2), 212–227.
Gallant, A.R., Rossi, P.E., Tauchen, G., 1993. Nonlinear dynamic structures. Econometrica 871–907.
Glosten, L.R., Jagannathan, R., Runkle, D.E., 1993. On the relation between the expected value and the volatility of the nominal excess return on stocks. J. Finance 48 (5), 1779–1801.
Hansen, P.R., Huang, Z., Shek, H.H., 2012. Realized GARCH: A joint model for returns and realized measures of volatility. J. Appl. Econometrics 27 (6), 877–906.
Hansen, P.R., Lunde, A., Nason, J.M., 2011. The model confidence set. Econometrica 79 (2), 453–497.
Hansen, P.R., Lunde, A., Voev, V., 2014. Realized beta GARCH: A multivariate GARCH model with realized measures of volatility. J. Appl. Econometrics 29 (5), 774–799.
He, C., Teräsvirta, T., 2002. An application of the analogy between vector ARCH and vector random coefficient autoregressive models. Working Paper.
Jeantheau, T., 1998. Strong consistency of estimators for multivariate ARCH models. Econometric Theory 14 (1), 70–86.
Kroner, K.F., Ng, V.K., 1998. Modeling asymmetric comovements of asset returns. Rev. Financ. Stud. 11 (4), 817–844.
McAleer, M., Hoti, S., Chan, F., 2009. Structure and asymptotic theory for multivariate asymmetric volatility. Econometric Rev. 28 (5), 422–440.
Nelson, D.B., 1991. Conditional heteroskedasticity in asset returns: A new approach. Econometrica 59 (2), 347–370.
Newey, W.K., McFadden, D., 1994. Large sample estimation and hypothesis testing. Handbook of Econometrics, Vol. 4. pp. 2111–2245.
Noureldin, D., Shephard, N., Sheppard, K., 2012. Multivariate high-frequency-based volatility (HEAVY) models. J. Appl. Econometrics 27 (6), 907–933.
Patton, A.J., 2011. Volatility forecast comparison using imperfect volatility proxies. J. Econometrics 160 (1), 246–256.
Patton, A.J., Sheppard, K., 2015. Good volatility, bad volatility: Signed jumps and the persistence of volatility. Rev. Econ. Stat. 97 (3), 683–697.
Pelletier, D., Kassi, A., 2014. The realized RSDC model. Working Paper.
Rivers, D., Vuong, Q., 2002. Model selection tests for nonlinear dynamic models. Econom. J. 5 (1), 1–39.
Rombouts, J., Laurent, S., Violante, F., 2013. On loss functions and ranking forecasting performances of multivariate volatility models. J. Econometrics 173 (1), 1–10.
Rombouts, J., Stentoft, L., Violante, F., 2014. The value of multivariate model sophistication: An application to pricing dow jones industrial average options. Int. J. Forecast. 30 (1), 78–98.
Shephard, N., Sheppard, K., 2010. Realising the future: Forecasting with high-frequency-based volatility (HEAVY) models. J. Appl. Econometrics 25 (2), 197–231.
Zakoïan, J.-M., 1994. Threshold heteroskedastic models. J. Econom. Dynam. Control 18 (5), 931–955.